Correlated electron-nuclear dynamics: Exact factorization of the molecular wavefunction

Ali Abedi,[1,2] Neepa T. Maitra,[3] and E. K. U. Gross[1,2]
[1]*Max-Planck Institut für Mikrostrukturphysik, Weinberg 2, D-06120 Halle, Germany*
[2]*European Theoretical Spectroscopy Facility (ETSF)*
[3]*Department of Physics and Astronomy, Hunter College and the City University of New York, 695 Park Avenue, New York, New York 10065, USA*

(Received 3 June 2012; accepted 31 July 2012; published online 27 August 2012)

It was recently shown [A. Abedi, N. T. Maitra, and E. K. U. Gross, Phys. Rev. Lett. **105**, 123002 (2010)] that the complete wavefunction for a system of electrons and nuclei evolving in a time-dependent external potential can be exactly factorized into an electronic wavefunction and a nuclear wavefunction. The concepts of an exact time-dependent potential energy surface (TDPES) and exact time-dependent vector potential emerge naturally from the formalism. Here, we present a detailed description of the formalism, including a full derivation of the equations that the electronic and nuclear wavefunctions satisfy. We demonstrate the relationship of this exact factorization to the traditional Born-Oppenheimer expansion. A one-dimensional model of the H_2^+ molecule in a laser field shows the usefulness of the exact TDPES in interpreting coupled electron-nuclear dynamics: we show how features of its structure indicate the mechanism of dissociation. We compare the exact TDPES with potential energy surfaces from the time-dependent Hartree-approach, and also compare traditional Ehrenfest dynamics with Ehrenfest dynamics on the exact TDPES. © *2012 American Institute of Physics*. [http://dx.doi.org/10.1063/1.4745836]

I. INTRODUCTION

The interplay of nuclear and electronic dynamics in the presence of time-dependent external fields leads to fascinating phenomena, especially beyond the perturbative regime, e.g., photo-induced molecular dissociation, charge-resonance enhanced ionization, control of electron localization, electron-hole migration after photo-excitation, to name a few.[2–6] The exact solution of the time-dependent Schrödinger equation (TDSE) is currently out of computational reach except for the very simplest of molecules,[7] such as H_2^+, so usually approximate methods are used. Typically, (but not always, see Refs. 8–11), these methods treat the nuclei classically as point charges with electron-nuclear coupling given by Ehrenfest dynamics, or surface-hopping;[12] a topical application is to model photochemical processes,[13,14] for example, in solar cells, to study the (field-free) dynamics ensuing after an initial electronic excitation. Indeed, several examples have shown that the predicted electron-hole migration can depend critically on the description of the nuclear motion and how it is correlated with the electronic dynamics (see Refs. 5 and 6 and references within). Apart from enabling calculations on more than the simplest systems possible, these methods provide much intuition, in particular, through the central concept of the potential energy surface (PES). Indeed, the very idea itself of surface-hopping would not exist without the notion of a landscape of coupled PESs. Dressed molecular potentials such as light-induced molecular potentials (LIMPS) (Ref. 15) have proven valuable in understanding processes such as bond-softening, stabilization against dissociation, etc., where the laser field induces avoided crossings between PESs. Approximate time-dependent potential energy surfaces (TDPES) were introduced by Kono[16] as instantaneous eigenvalues of the electronic Hamiltonian, and have proven extremely useful in the interpretation of system-field phenomena, as have the quasi-static or phase-adiabatic PES's used recently to interpret electron localization in dissociative ionization.[17] Recent work of Cederbaum[18] introduced a TDPES in a different way, by generalizing the Born-Oppenheimer (BO) approximation to include time-dependent external potentials. In short, the PES is perhaps the most central concept in our understanding of molecular motion.

In a recent Letter,[1] we showed that an *exact* TDPES may be defined, via a rigorous separation of electronic and nuclear motion by introducing an *exact* factorization of the full electron-nuclear wavefunction. The idea of an exact factorization was first introduced by Hunter[19] for the static case. He also deduced the exact equation of motion for the nuclear factor. The equation of motion for the electronic wavefunction was first given by Gidopoulos and Gross[20] for the time-independent case. Both in the static and in the time-dependent cases, the factorization leads to an exact definition of the PES, and also of the Berry vector potential. What is particularly interesting about the vector potential is that Berry-Pancharatnam phases[21] are usually interpreted as arising from some *approximation* where a system is decoupled from "the rest of the world," thereby making the system Hamiltonian dependent on some "environmental" parameters. For example, in the static BO approximation, the electronic Hamiltonian depends parametrically on nuclear positions, and when the molecular wavefunction is approximated by a single product of a nuclear wavefunction and an eigenstate of the

electronic Hamiltonian, the equation of motion for the former contains a Berry vector potential. The question whether the BO Berry phase survives in the exact treatment was first discussed in Ref. 20 for the static case and in Ref. 1 for the time-dependent case.

In the present paper, we provide the detailed derivation of the formalism of Ref. 1 (Sec. II), analyse features of the exact electron-nuclear coupling terms in general (Sec. III), including their relationship to couplings in the traditional Born-Oppenheimer expansion, and then study the TDPES for the specific case of a model H_2^+ molecule in an oscillating electric field (Sec. IV). The remainder of this introduction serves to set up the problem at hand, and to remind the reader of the Born-Oppenheimer treatment of the electron-nuclear system.

A. The Hamiltonian

In this section, we establish notation and define the Hamiltonian for the combined system of electrons and nuclei. The coordinates of the N_e electrons are collectively denoted by $\underline{\underline{\mathbf{r}}}\underline{\underline{\mathbf{s}}}$ where $\underline{\underline{\mathbf{r}}} \equiv \{r_j\}$ and $\underline{\underline{\mathbf{s}}} \equiv \{s_j\}$, $j = 1 \ldots N_e$, represent electronic spatial and spin coordinates, respectively. The N_n nuclei have masses $M_1 \ldots M_{N_n}$ and charges $Z_1 \ldots Z_{N_n}$ and coordinates collectively denoted by $\underline{\underline{\mathbf{R}}}\underline{\underline{\sigma}}$, where $\underline{\underline{\mathbf{R}}} \equiv \{R_\alpha\}$ and $\underline{\underline{\sigma}} \equiv \{\sigma_\alpha\}$, $\alpha = 1 \ldots N_n$, represent nuclear spatial and spin coordinates, respectively. Furthermore, we consider that the system is under the influence of some time-dependent external scalar field. The system is described, non-relativistically, by the Hamiltonian

$$\hat{H} = \hat{H}_{BO}(\underline{\underline{\mathbf{r}}}, \underline{\underline{\mathbf{R}}}) + \hat{V}^e_{\text{ext}}(\underline{\underline{\mathbf{r}}}, t) + \hat{T}_n(\underline{\underline{\mathbf{R}}}) + \hat{V}^n_{\text{ext}}(\underline{\underline{\mathbf{R}}}, t), \quad (1)$$

where $\hat{H}_{BO}(\underline{\underline{\mathbf{r}}}, \underline{\underline{\mathbf{R}}})$ is the familiar Born-Oppenheimer electronic Hamiltonian

$$\hat{H}_{BO} = \hat{T}_e(\underline{\underline{\mathbf{r}}}) + \hat{W}_{ee}(\underline{\underline{\mathbf{r}}}) + \hat{W}_{en}(\underline{\underline{\mathbf{r}}}, \underline{\underline{\mathbf{R}}}) + \hat{W}_{nn}(\underline{\underline{\mathbf{R}}}). \quad (2)$$

The subscripts "e" and "n" refer to electrons and nuclei, respectively, and atomic units are used throughout ($e^2 = \hbar = m_e = 1$). Here,

$$\hat{T}_e = -\sum_{j=1}^{N_e} \frac{1}{2}\nabla_j^2, \quad (3)$$

and

$$\hat{T}_n = -\sum_{\alpha=1}^{N_n} \frac{1}{2M_\alpha}\nabla_\alpha^2, \quad (4)$$

denote the kinetic-energy operators of the electrons and nuclei, respectively. All external scalar potentials on the system (e.g., electric fields) are represented by

$$\hat{V}^n_{\text{ext}} = \sum_{\alpha}^{N_n} v^n_{\text{ext}}(\mathbf{R}_\alpha, t), \quad (5)$$

and

$$\hat{V}^e_{\text{ext}} = \sum_{j}^{N_e} v^e_{\text{ext}}(\mathbf{r}_j, t). \quad (6)$$

The particle-particle Coulomb interactions have the form

$$\hat{W}_{nn} = \frac{1}{2}\sum_{\substack{\alpha,\beta=1 \\ \alpha\neq\beta}}^{N_n} \frac{Z_\alpha Z_\beta}{|\mathbf{R}_\alpha - \mathbf{R}_\beta|}, \quad (7)$$

$$\hat{W}_{ee} = \frac{1}{2}\sum_{\substack{i,j=1 \\ i\neq j}}^{N_e} \frac{1}{|\mathbf{r}_i - \mathbf{r}_j|}, \quad (8)$$

$$\hat{W}_{en} = -\sum_{j}^{N_e}\sum_{\alpha}^{N_n} \frac{Z_\alpha}{|\mathbf{r}_j - \mathbf{R}_\alpha|}. \quad (9)$$

The quantum mechanical equation of motion of such a system is given by the TDSE

$$\hat{H}\Psi(\underline{\underline{\mathbf{r}}}\underline{\underline{\mathbf{s}}}, \underline{\underline{\mathbf{R}}}\underline{\underline{\sigma}}, t) = i\partial_t\Psi(\underline{\underline{\mathbf{r}}}\underline{\underline{\mathbf{s}}}, \underline{\underline{\mathbf{R}}}\underline{\underline{\sigma}}, t). \quad (10)$$

The full electron-nuclear wavefunction, $\Psi(\underline{\underline{\mathbf{r}}}\underline{\underline{\mathbf{s}}}, \underline{\underline{\mathbf{R}}}\underline{\underline{\sigma}}, t)$, that satisfies the TDSE (10), contains the complete information on the system. As discussed in the Introduction, it can be solved numerically only for very small systems of one or two electrons and nuclei and, moreover, Ψ does not give access to PESs, which provide an intuitive understanding and interpretation of the coupled electron-nuclear dynamics.

B. The Born-Oppenheimer approximation

The Born-Oppenheimer approximation is among the most basic approximations in the quantum theory of molecules and solids. Consider the case when there is no external time-dependence in the Hamiltonian. The BO approximation relies on the fact that electrons typically move much faster than the nuclei; on the timescale of nuclear motion, the electrons "instantly" adjust to remain on the instantaneous eigenstate. This "adiabatic approximation" allows us to visualize a molecule or solid as a set of nuclei moving on the PES generated by the electrons in a specific electronic eigenstate. The electronic Hamiltonian $\hat{H}_{BO}(\underline{\underline{\mathbf{r}}}, \underline{\underline{\mathbf{R}}})$ depends parametrically on the nuclear positions, via the electron-nuclear Coulomb interaction. That is, the stationary electronic Schrödinger equation is solved for each fixed nuclear configuration $\underline{\underline{\mathbf{R}}}\underline{\underline{\sigma}}$,

$$\hat{H}_{BO}(\underline{\underline{\mathbf{r}}}, \underline{\underline{\mathbf{R}}})\phi^j_{\underline{\underline{\mathbf{R}}}\underline{\underline{\sigma}}}(\underline{\underline{\mathbf{r}}}\underline{\underline{\mathbf{s}}}) = V^j_{BO}(\underline{\underline{\mathbf{R}}}\underline{\underline{\sigma}})\phi^j_{\underline{\underline{\mathbf{R}}}\underline{\underline{\sigma}}}(\underline{\underline{\mathbf{r}}}\underline{\underline{\mathbf{s}}}), \quad (11)$$

yielding $(\underline{\underline{\mathbf{R}}}\underline{\underline{\sigma}})$-dependent eigenvalues $V^j_{BO}(\underline{\underline{\mathbf{R}}}\underline{\underline{\sigma}})$ and eigenfunctions $\phi^j_{\underline{\underline{\mathbf{R}}}\underline{\underline{\sigma}}}$. The total molecular wavefunction, $\Psi_{BO}(\underline{\underline{\mathbf{r}}}\underline{\underline{\mathbf{s}}}, \underline{\underline{\mathbf{R}}}\underline{\underline{\sigma}})$, is then approximated as a product of the relevant electronic state, $\phi^j_{\underline{\underline{\mathbf{R}}}\underline{\underline{\sigma}}}(\underline{\underline{\mathbf{r}}}\underline{\underline{\mathbf{s}}})$, and a nuclear wavefunction $\chi^{BO}_{j\nu}(\underline{\underline{\mathbf{R}}}\underline{\underline{\sigma}})$ satisfying the corresponding BO nuclear Schrödinger equation

$$\left(\sum_{\alpha=1}^{N_n}\frac{1}{2M_\alpha}\left(-i\nabla_\alpha + \mathcal{F}^{BO}_{jj,\alpha}(\underline{\underline{\mathbf{R}}}\underline{\underline{\sigma}})\right)^2 + \epsilon^j_{BO}(\underline{\underline{\mathbf{R}}}\underline{\underline{\sigma}})\right)\chi^{BO}_{j\nu}(\underline{\underline{\mathbf{R}}}\underline{\underline{\sigma}}) = E\chi^{BO}_{j\nu}(\underline{\underline{\mathbf{R}}}\underline{\underline{\sigma}}), \quad (12)$$

where

$$\epsilon^{j}_{BO}(\underline{\underline{\mathbf{R}}}\underline{\underline{\sigma}}) = \sum_{\underline{\underline{\mathbf{s}}}} \left\langle \phi^{j}_{\underline{\underline{\mathbf{R}}}\underline{\underline{\sigma}}} \right| \hat{H}_{BO}(\underline{\mathbf{r}}, \underline{\underline{\mathbf{R}}}) + \sum_{\alpha} \frac{\left(-i\nabla_{\alpha} - \mathcal{F}^{BO}_{jj,\alpha}\right)^2}{2M_{\alpha}} \left| \phi^{j}_{\underline{\underline{\mathbf{R}}}\underline{\underline{\sigma}}} \right\rangle_{\underline{\mathbf{r}}}, \tag{13}$$

and

$$\mathcal{F}^{BO}_{jj,\alpha}(\underline{\underline{\mathbf{R}}}\underline{\underline{\sigma}}) = -i \sum_{\underline{\underline{\mathbf{s}}}} \langle \phi^{j}_{\underline{\underline{\mathbf{R}}}\underline{\underline{\sigma}}} | \nabla_{\alpha} \phi^{j}_{\underline{\underline{\mathbf{R}}}\underline{\underline{\sigma}}} \rangle_{\underline{\mathbf{r}}}, \tag{14}$$

where $\langle .. | .. \rangle_{\underline{\mathbf{r}}}$ indicates an inner product over spatial electronic variables only. The index ν of the nuclear wave function labels the vibrational/rotational eigenstate on the jth PES. The second term on the right of Eq. (13) is often referred to as the "BO diagonal correction" or "adiabatic correction." The potential energy surface $\epsilon^{j}_{BO}(\underline{\underline{\mathbf{R}}}\underline{\underline{\sigma}})$ is enormously important in molecular physics and quantum chemistry. It is a central tool in the analysis and interpretation of molecular absorption and emission spectra, experiments involving nuclear motion, mechanisms of dissociation, energy-transfer, for example. The nuclear dynamics on a *single* PES (sometimes called "BO dynamics") is obtained by using the Hamiltonian on the left of Eq. (12) in a time-dependent Schrödinger equation for a time-dependent nuclear wavefunction $\chi(\underline{\underline{\mathbf{R}}}\underline{\underline{\sigma}}, t)$. This corresponds to approximating the total molecular wavefunction by a time-dependent nuclear wavepacket multiplied with a static electronic BO state

$$\Psi(\underline{\underline{\mathbf{r}}}\underline{\underline{\mathbf{s}}}, \underline{\underline{\mathbf{R}}}\underline{\underline{\sigma}}, t) \approx \chi^{BO}(\underline{\underline{\mathbf{R}}}\underline{\underline{\sigma}}, t) \phi^{j}_{\underline{\underline{\mathbf{R}}}\underline{\underline{\sigma}}}(\underline{\underline{\mathbf{r}}}\underline{\underline{\mathbf{s}}}). \tag{15}$$

The vector potential $\mathcal{F}^{BO}_{jj,\alpha}(\underline{\underline{\mathbf{R}}}\underline{\underline{\sigma}})$, especially the Berry phase associated with it, $\oint \mathcal{F}^{BO}_{jj,\alpha}(\underline{\underline{\mathbf{R}}}\underline{\underline{\sigma}}) \cdot d\underline{\underline{\mathbf{R}}}$, captures the essential features of the behavior of a system with conical intersections. Inclusion of the Berry phase can significantly shift and re-order the energy eigenvalues of molecular roto-vibrational spectra, as well as scattering cross-sections (although sometimes undetected in experiments that measure integrated quantities, due to cancellations between paths, see e.g., Refs. 22–26 and references within).

It appears from the above discussion that in the traditional treatment of molecules and solids, the concepts of the PES and the Berry phase arise as a consequence of the BO approximation. Some of the most fascinating phenomena of condensed-matter physics, such as superconductivity, however, appear in the regime where the BO approximation is not valid; likewise, typical photodynamical processes in molecules require going beyond the single-electronic-surface picture. This raises the question: If one were to solve the Schrödinger equation of the full electron-nuclear Hamiltonian exactly (i.e., beyond the BO approximation), do the Berry phase and the potential energy surface survive, with a possibly modified form, and if so, how and where do they show up? What is their relation to the traditional potential energy surface and Berry phase in the BO approximation? Moreover, many interesting phenomena occur when molecules or solids are exposed to time-dependent external fields, e.g., lasers. Can one give a precise meaning to a *time-dependent* potential energy surface and a time-dependent vector potential?

Before answering the points raised above, focussing on the time-dependent case, we briefly discuss the Born-Oppenheimer *expansion*, which solves the full TDSE Eq. (10) exactly for the coupled electron-nuclear system.

C. The Born-Oppenheimer expansion

The set of electronic eigenfunctions $\{\phi^{j}_{\underline{\underline{\mathbf{R}}}\underline{\underline{\sigma}}}(\underline{\underline{\mathbf{r}}}\underline{\underline{\mathbf{s}}})\}$ calculated from Eq. (11) form a complete orthonormal set in the electronic space for each fixed $\underline{\underline{\mathbf{R}}}\underline{\underline{\sigma}}$,

$$\sum_{\underline{\underline{\mathbf{s}}}} \int d\underline{\underline{\mathbf{r}}} \phi^{l*}_{\underline{\underline{\mathbf{R}}}\underline{\underline{\sigma}}}(\underline{\underline{\mathbf{r}}}\underline{\underline{\mathbf{s}}}) \phi^{j}_{\underline{\underline{\mathbf{R}}}\underline{\underline{\sigma}}}(\underline{\underline{\mathbf{r}}}\underline{\underline{\mathbf{s}}}) = \delta_{lj}, \tag{16}$$

therefore, the total time-dependent wavefunction of the system $\Psi(\underline{\underline{\mathbf{r}}}\underline{\underline{\mathbf{s}}}, \underline{\underline{\mathbf{R}}}\underline{\underline{\sigma}}, t)$ can be expanded in that basis

$$\Psi(\underline{\underline{\mathbf{r}}}\underline{\underline{\mathbf{s}}}, \underline{\underline{\mathbf{R}}}\underline{\underline{\sigma}}, t) = \sum_{j=1}^{\infty} \chi^{BO}_{j}(\underline{\underline{\mathbf{R}}}\underline{\underline{\sigma}}, t) \phi^{j}_{\underline{\underline{\mathbf{R}}}\underline{\underline{\sigma}}}(\underline{\underline{\mathbf{r}}}\underline{\underline{\mathbf{s}}}). \tag{17}$$

Here,

$$\chi^{BO}_{j}(\underline{\underline{\mathbf{R}}}\underline{\underline{\sigma}}, t) = \sum_{\underline{\underline{\mathbf{s}}}} \int d\underline{\underline{\mathbf{r}}} \phi^{j*}_{\underline{\underline{\mathbf{R}}}\underline{\underline{\sigma}}}(\underline{\underline{\mathbf{r}}}\underline{\underline{\mathbf{s}}}) \Psi(\underline{\underline{\mathbf{r}}}\underline{\underline{\mathbf{s}}}, \underline{\underline{\mathbf{R}}}\underline{\underline{\sigma}}, t) \tag{18}$$

are the expansion coefficients, which are functions of the nuclear degrees of freedom and time. Equation (17) is the so-called BO expansion, which is an *exact* representation of the complete molecular wavefunction due to the completeness of $\{\phi^{j}_{\underline{\underline{\mathbf{R}}}\underline{\underline{\sigma}}}(\underline{\underline{\mathbf{r}}}\underline{\underline{\mathbf{s}}})\}$. It applies also to fully-time-dependent problems where Ψ evolves under external time-dependent potentials $\hat{V}^{e}_{\text{ext}}$. In practice, for numerically feasible calculations, approximations are introduced to limit the expansion to a small subset of $\{\phi^{j}_{\underline{\underline{\mathbf{R}}}\underline{\underline{\sigma}}}(\underline{\underline{\mathbf{r}}}\underline{\underline{\mathbf{s}}})\}$. By inserting the expansion (17) into Eq. (10), multiplying by $\phi^{j*}_{\underline{\underline{\mathbf{R}}}\underline{\underline{\sigma}}}(\underline{\underline{\mathbf{r}}}\underline{\underline{\mathbf{s}}})$ from the left, and integrating over the electronic degrees of freedom, equations for the expansion coefficients $\chi^{BO}_{j}(\underline{\underline{\mathbf{R}}}\underline{\underline{\sigma}}, t)$ are determined. One obtains

$$\left[\sum_{\alpha} \frac{1}{2M_{\alpha}} \left(-i\nabla_{\alpha} + \mathcal{F}^{BO}_{kk,\alpha}\right)^2 + \hat{V}^{n}_{\text{ext}} + \epsilon^{k}_{BO}\right] \chi^{BO}_{k} + \sum_{j \neq k} \left[\langle \phi^{k} | \hat{V}^{e}_{\text{ext}}(t) | \phi^{j} \rangle - \sum_{\alpha} \Lambda^{BO}_{kj,\alpha}\right] \chi^{BO}_{j} = i \frac{\partial \chi^{BO}_{k}}{\partial t}. \tag{19}$$

Here,

$$\epsilon^{k}_{BO}(\underline{\underline{\mathbf{R}}}\underline{\underline{\sigma}}, t) = \sum_{\underline{\sigma}} \langle \phi^{k}_{\underline{\underline{\mathbf{R}}}\underline{\underline{\sigma}}} | \hat{H}_{BO} + \hat{V}^{e}_{\text{ext}} + \sum_{\alpha} \frac{\left(-i\nabla_{\alpha} - \mathcal{F}^{BO}_{kk,\alpha}\right)^2}{2M_{\alpha}} \left| \phi^{k}_{\underline{\underline{\mathbf{R}}}\underline{\underline{\sigma}}} \right\rangle_{\underline{\mathbf{r}}} \tag{20}$$

is the time-dependent scalar potential and is the kth generalized BO potential energy, generalized to account for the time-dependent external field (cf. Eq. (13)). The terms

$$\Lambda^{BO}_{kj,\alpha}(\underline{\underline{\mathbf{R}}}) = \frac{1}{2M_{\alpha}} \left[\mathcal{G}^{BO}_{kj,\alpha}(\underline{\underline{\mathbf{R}}}) + 2\mathcal{F}^{BO}_{kj,\alpha}(\underline{\underline{\mathbf{R}}}) \cdot (i\nabla_{\alpha})\right] \tag{21}$$

are called the "nonadiabatic couplings," defined by[27–29]

$$\mathcal{F}^{BO}_{kj,\alpha}(\underline{\underline{\mathbf{R}}}) = -i\langle\phi^k_{\underline{\underline{\mathbf{R}}}\sigma}|\nabla_\alpha\phi^j_{\underline{\underline{\mathbf{R}}}\sigma}\rangle,$$
$$\mathcal{G}^{BO}_{kj,\alpha}(\underline{\underline{\mathbf{R}}}) = \langle\phi^k_{\underline{\underline{\mathbf{R}}}\sigma}|\nabla^2_\alpha\phi^j_{\underline{\underline{\mathbf{R}}}\sigma}\rangle. \quad (22)$$

II. EXACT FACTORIZATION OF THE TIME-DEPENDENT ELECTRON-NUCLEAR WAVEFUNCTION

The BO expansion Eq. (17) yields the complete molecular wavefunction exactly. Instead of having an infinite sum of terms involving an infinite set of generalized PES's and nonadiabatic couplings, the question arises whether it is possible to represent the complete, time-dependent, electron-nuclear wavefunction exactly as a *single* product of an electronic wavefunction and a nuclear wavefunction. In this section, we show that the answer is yes. We derive formally exact equations of motion for each subsystem, out of which emerge rigorous definitions of a time-dependent potential energy surface (TDPES) and a time-dependent vector potential.

Visually, the decomposition is similar in form to the single-surface BO approximation, yet it is exact. There is no assumption on the time scale of the motions of each subsystem, i.e., unlike in the BO approximation, we do not solve for the "fast" variables first and then feed it into the equation for the "slower" variables. Instead, the equations of motion for each subsystem are derived together, in a variational approach. The exact decomposition, contrary to the BO separation, accounts for the full correlation between the two subsystems, regardless of the mass and energy of the nuclear subsystem. In the following, we formalize the idea as a theorem, which we then prove. We discuss in detail the implications of this exact decomposition.

A. The exact factorization

Theorem I. (a): *The exact solution of Eq. (10) can be written as a single product*

$$\Psi(\underline{\underline{\mathbf{r}}}\underline{\underline{\mathbf{s}}}, \underline{\underline{\mathbf{R}}}\underline{\underline{\sigma}}, t) = \Phi_{\underline{\underline{\mathbf{R}}}\underline{\underline{\sigma}}}(\underline{\underline{\mathbf{r}}}\underline{\underline{\mathbf{s}}}, t)\chi(\underline{\underline{\mathbf{R}}}\underline{\underline{\sigma}}, t), \quad (23)$$

where $\Phi_{\underline{\underline{\mathbf{R}}}\underline{\underline{\sigma}}}(\underline{\underline{\mathbf{r}}}\underline{\underline{\mathbf{s}}}, t)$ *satisfies the Partial Normalization Condition (PNC),*

$$\sum_{\underline{\underline{\mathbf{s}}}}\int d\underline{\underline{\mathbf{r}}}|\Phi_{\underline{\underline{\mathbf{R}}}\underline{\underline{\sigma}}}(\underline{\underline{\mathbf{r}}}\underline{\underline{\mathbf{s}}}, t)|^2 = 1, \quad (24)$$

for any fixed nuclear configuration, $\underline{\underline{\mathbf{R}}}\underline{\underline{\sigma}}$*, at any time t.*

The PNC is critical in making this theorem meaningful: Eq. (23) on its own would be rather meaningless, because, for example, one could then simply just take $\chi(\underline{\underline{\mathbf{R}}}\underline{\underline{\sigma}}, t) \equiv 1$. In fact, one can come up with many different decompositions that satisfy Eq. (23) but that violate the PNC Eq. (24); it is the latter that makes the decomposition unique up to a gauge-like transformation, as we shall see shortly in Sec. II B. We will also see there that it is the PNC that allows the interpretation of $\Phi_{\underline{\underline{\mathbf{R}}}\underline{\underline{\sigma}}}(\underline{\underline{\mathbf{r}}}\underline{\underline{\mathbf{s}}}, t)$ as a conditional probability amplitude, and $\chi(\underline{\underline{\mathbf{R}}}\underline{\underline{\sigma}}, t)$ as a marginal probability amplitude, leading to their identification as electronic and nuclear wavefunctions, respectively. First, we prove Part (a) of Theorem I.

Proof: Given $\Psi(\underline{\underline{\mathbf{r}}}\underline{\underline{\mathbf{s}}}, \underline{\underline{\mathbf{R}}}\underline{\underline{\sigma}}, t)$, the exact solution of the full TDSE (10), we choose $\chi(\underline{\underline{\mathbf{R}}}\underline{\underline{\sigma}}, t)$ and $\Phi_{\underline{\underline{\mathbf{R}}}\underline{\underline{\sigma}}}(\underline{\underline{\mathbf{r}}}\underline{\underline{\mathbf{s}}}, t)$, at any instant in time, as

$$\chi(\underline{\underline{\mathbf{R}}}\underline{\underline{\sigma}}, t) = e^{iS(\underline{\underline{\mathbf{R}}}\underline{\underline{\sigma}}, t)}\sqrt{\textstyle\sum_{\underline{\underline{\mathbf{s}}}}\int d\underline{\underline{\mathbf{r}}}|\Psi(\underline{\underline{\mathbf{r}}}\underline{\underline{\mathbf{s}}}, \underline{\underline{\mathbf{R}}}\underline{\underline{\sigma}}, t)|^2}, \quad (25)$$

and

$$\Phi_{\underline{\underline{\mathbf{R}}}\underline{\underline{\sigma}}}(\underline{\underline{\mathbf{r}}}\underline{\underline{\mathbf{s}}}, t) = \Psi(\underline{\underline{\mathbf{r}}}\underline{\underline{\mathbf{s}}}, \underline{\underline{\mathbf{R}}}\underline{\underline{\sigma}}, t)/\chi(\underline{\underline{\mathbf{R}}}\underline{\underline{\sigma}}, t), \quad (26)$$

where $S(\underline{\underline{\mathbf{R}}}\underline{\underline{\sigma}}, t)$ is real. The PNC Eq. (24) then follows immediately

$$\sum_{\underline{\underline{\mathbf{s}}}}\int d\underline{\underline{\mathbf{r}}}|\Phi_{\underline{\underline{\mathbf{R}}}\underline{\underline{\sigma}}}(\underline{\underline{\mathbf{r}}}\underline{\underline{\mathbf{s}}}, t)|^2 = \frac{\sum_{\underline{\underline{\mathbf{s}}}}\int d\underline{\underline{\mathbf{r}}}|\Psi(\underline{\underline{\mathbf{r}}}\underline{\underline{\mathbf{s}}}, \underline{\underline{\mathbf{R}}}\underline{\underline{\sigma}}, t)|^2}{|\chi(\underline{\underline{\mathbf{R}}}\underline{\underline{\sigma}}, t)|^2},$$
$$= \frac{|\chi(\underline{\underline{\mathbf{R}}}\underline{\underline{\sigma}}, t)|^2}{|\chi(\underline{\underline{\mathbf{R}}}\underline{\underline{\sigma}}, t)|^2} = 1. \quad (27)$$

This concludes the proof of Theorem I (a). It will become clear throughout this paper that, in many respects, the nuclear factor $\chi(\underline{\underline{\mathbf{R}}}\underline{\underline{\sigma}}, t)$ can be viewed as a proper nuclear wavefunction. Like in the static case,[20] introducing the phase factor in Eq. (25) allows $\chi(\underline{\underline{\mathbf{R}}}\underline{\underline{\sigma}}, t)$ to have the correct antisymmetry if the nuclear subsystem contains identical fermionic nuclei.

Next comes the question; what equations do $\Phi_{\underline{\underline{\mathbf{R}}}\underline{\underline{\sigma}}}(\underline{\underline{\mathbf{r}}}\underline{\underline{\mathbf{s}}}, t)$ and $\chi(\underline{\underline{\mathbf{R}}}\underline{\underline{\sigma}}, t)$ satisfy? The answer entails the second part of Theorem I.

Theorem I (b): *The wavefunctions* $\Phi_{\underline{\underline{\mathbf{R}}}\underline{\underline{\sigma}}}(\underline{\underline{\mathbf{r}}}\underline{\underline{\mathbf{s}}}, t)$ *and* $\chi(\underline{\underline{\mathbf{R}}}\underline{\underline{\sigma}}, t)$ *satisfy*

$$\left(\hat{H}_{el}(\underline{\underline{\mathbf{r}}}\underline{\underline{\mathbf{s}}}, \underline{\underline{\mathbf{R}}}\underline{\underline{\sigma}}, t) - \epsilon(\underline{\underline{\mathbf{R}}}\underline{\underline{\sigma}}, t)\right)\Phi_{\underline{\underline{\mathbf{R}}}\underline{\underline{\sigma}}}(\underline{\underline{\mathbf{r}}}\underline{\underline{\mathbf{s}}}, t) = i\,\partial_t\Phi_{\underline{\underline{\mathbf{R}}}\underline{\underline{\sigma}}}(\underline{\underline{\mathbf{r}}}\underline{\underline{\mathbf{s}}}, t), \quad (28)$$

$$\left(\sum_{\alpha=1}^{N_n}\frac{1}{2M_\alpha}(-i\nabla_\alpha + \mathbf{A}_\alpha(\underline{\underline{\mathbf{R}}}\underline{\underline{\sigma}}, t))^2 + \hat{V}^n_{\text{ext}}(\underline{\underline{\mathbf{R}}}, t) + \epsilon(\underline{\underline{\mathbf{R}}}\underline{\underline{\sigma}}, t)\right)$$
$$\times\,\chi(\underline{\underline{\mathbf{R}}}\underline{\underline{\sigma}}, t) = i\,\partial_t\chi(\underline{\underline{\mathbf{R}}}\underline{\underline{\sigma}}, t), \quad (29)$$

where the electronic Hamiltonian is

$$\hat{H}_{el}(\underline{\underline{\mathbf{r}}}\underline{\underline{\mathbf{s}}}, \underline{\underline{\mathbf{R}}}\underline{\underline{\sigma}}, t) = \hat{H}_{BO}(\underline{\mathbf{r}}, \underline{\mathbf{R}}, t) + \hat{V}^e_{\text{ext}}(\underline{\mathbf{r}}, t) + \hat{U}^{coup}_{en}[\Phi_{\underline{\underline{\mathbf{R}}}\underline{\underline{\sigma}}}, \chi]. \quad (30)$$

Here, the electron-nuclear coupling potential $\hat{U}^{coup}_{en}[\Phi_{\underline{\underline{\mathbf{R}}}\underline{\underline{\sigma}}}, \chi]$*, scalar potential* $\epsilon(\underline{\underline{\mathbf{R}}}\underline{\underline{\sigma}}, t)$*, and vector potential* $\mathbf{A}_\alpha(\underline{\underline{\mathbf{R}}}\underline{\underline{\sigma}}, t)$ *terms are*

$$\hat{U}^{coup}_{en}[\Phi_{\underline{\underline{\mathbf{R}}}\underline{\underline{\sigma}}}, \chi]$$
$$= \sum_{\alpha=1}^{N_n}\frac{1}{M_\alpha}\left[\frac{(-i\nabla_\alpha - \mathbf{A}_\alpha(\underline{\underline{\mathbf{R}}}\underline{\underline{\sigma}}, t))^2}{2}\right.$$
$$\left. + \left(\frac{-i\nabla_\alpha\chi(\underline{\underline{\mathbf{R}}}\underline{\underline{\sigma}}, t)}{\chi(\underline{\underline{\mathbf{R}}}\underline{\underline{\sigma}}, t)} + \mathbf{A}_\alpha(\underline{\underline{\mathbf{R}}}\underline{\underline{\sigma}}, t)\right)\cdot(-i\nabla_\alpha - \mathbf{A}_\alpha(\underline{\underline{\mathbf{R}}}\underline{\underline{\sigma}}, t))\right], \quad (31)$$

$$\epsilon(\underline{\underline{\mathbf{R}}}\underline{\underline{\sigma}}, t) = \sum_{\underline{\underline{\mathbf{s}}}}\langle\Phi_{\underline{\underline{\mathbf{R}}}\underline{\underline{\sigma}}}(t)|\hat{H}_{el}((\underline{\underline{\mathbf{r}}}\underline{\underline{\mathbf{s}}}, \underline{\underline{\mathbf{R}}}\underline{\underline{\sigma}}, t) - i\,\partial_t|\Phi_{\underline{\underline{\mathbf{R}}}\underline{\underline{\sigma}}}(t)\rangle_{\underline{\mathbf{r}}}, \quad (32)$$

$$\mathbf{A}_\alpha(\underline{\underline{\mathbf{R}}}\underline{\underline{\sigma}}, t) = \sum_{\underline{\underline{\mathbf{s}}}}\langle\Phi_{\underline{\underline{\mathbf{R}}}\underline{\underline{\sigma}}}(t)| - i\nabla_\alpha\Phi_{\underline{\underline{\mathbf{R}}}\underline{\underline{\sigma}}}(t)\rangle_{\underline{\mathbf{r}}}, \quad (33)$$

where $\langle ..|..|..\rangle_{\underline{\underline{\mathbf{r}}}}$ *denotes an inner product over all spatial electronic variables only.*

Proof: In order to derive the equations of motion for $\Phi_{\underline{\underline{\mathbf{R}}}\sigma}(\underline{\underline{\mathbf{r}}}\underline{\underline{\mathbf{s}}}, t)$ and $\chi(\underline{\underline{\mathbf{R}}}\underline{\underline{\sigma}}, t)$, we follow the strategy employed in the static case (see Ref. 20), i.e., we plug the product ansatz in the variational principle and search for the stationary point. Afterwards, we prove: if $\Phi_{\underline{\underline{\mathbf{R}}}\sigma}(\underline{\underline{\mathbf{r}}}\underline{\underline{\mathbf{s}}}, t)$ and $\chi(\underline{\underline{\mathbf{R}}}\underline{\underline{\sigma}}, t)$ are the solutions of Eqs. (28) and (29), then $\Phi_{\underline{\underline{\mathbf{R}}}\sigma}(\underline{\underline{\mathbf{r}}}\underline{\underline{\mathbf{s}}}, t)\chi(\underline{\underline{\mathbf{R}}}\underline{\underline{\sigma}}, t)$ is the solution of TDSE (10). We begin the derivation by briefly reviewing Frenkel's stationary action principle as this is the key instrument to derive the equations of motion for each subsystem.

The quantum mechanical action is defined as

$$\mathcal{S}[\Psi, \Psi^*] = \int_{t_i}^{t_f} dt \langle \Psi | \hat{H} - i\partial_t | \Psi \rangle, \tag{34}$$

a functional of the time-dependent wavefunction $\Psi(t)$ and its complex conjugate. The equation of motion of the quantum system, the TDSE of Eq. (10), is obtained by requiring the variation of the action $\mathcal{S}$ with respect to all wavefunctions $\Psi(t)$ that satisfy the boundary condition

$$\delta\Psi(t_i) = \delta\Psi(t_f) = 0, \tag{35}$$

to be stationary, i.e.,

$$\delta_{\Psi^*}\mathcal{S} = 0. \tag{36}$$

Now we apply this general variational principle to our problem in the following way. We insert the product wavefunction in the action functional (34), with Hamiltonian given by Eq. (1), rewriting it as

$$\mathcal{S}[\Phi_{\underline{\underline{\mathbf{R}}}\sigma}, \Phi^*_{\underline{\underline{\mathbf{R}}}\sigma}, \chi, \chi^*] = \sum_{\underline{\underline{\mathbf{s}}},\underline{\underline{\sigma}}} \int_{t_i}^{t_f} dt \int d\underline{\underline{\mathbf{R}}} \int d\underline{\underline{\mathbf{r}}} \Bigg[|\chi|^2 \Phi^*_{\underline{\underline{\mathbf{R}}}\sigma} \left(\hat{H}_{BO} + \hat{V}^e_{\text{ext}} + \sum_\alpha \frac{-\nabla^2_\alpha}{2M_\alpha} - i\partial_t \right) \Phi_{\underline{\underline{\mathbf{R}}}\sigma}$$
$$+ |\Phi_{\underline{\underline{\mathbf{R}}}\sigma}|^2 \chi^* \left(\sum_\alpha \frac{-\nabla^2_\alpha}{2M_\alpha} + \hat{V}^n_{\text{ext}} - i\partial_t \right) \chi + |\chi|^2 \Phi^*_{\underline{\underline{\mathbf{R}}}\sigma} \sum_\alpha \frac{1}{M_\alpha} (-i\nabla_\alpha \chi/\chi) \cdot (-i\nabla_\alpha \Phi_{\underline{\underline{\mathbf{R}}}\sigma}) \Bigg]. \tag{37}$$

The equations of motion for $\Phi_{\underline{\underline{\mathbf{R}}}\sigma}(\underline{\underline{\mathbf{r}}}\underline{\underline{\mathbf{s}}}, t)$ and $\chi(\underline{\underline{\mathbf{R}}}\underline{\underline{\sigma}}, t)$ are obtained by requiring the action functional (37) to be stationary with respect to variations of each wavefunction subject to the PNC (24), i.e.,

$$\frac{\delta\mathcal{S}[\Phi_{\underline{\underline{\mathbf{R}}}\sigma}, \Phi^*_{\underline{\underline{\mathbf{R}}}\sigma}, \chi, \chi^*]}{\delta\Phi^*_{\underline{\underline{\mathbf{R}}}\sigma}(\underline{\underline{\mathbf{r}}}\underline{\underline{\mathbf{s}}}, t)} = 0, \text{ and } \frac{\delta\mathcal{S}[\Phi_{\underline{\underline{\mathbf{R}}}\sigma}, \Phi^*_{\underline{\underline{\mathbf{R}}}\sigma}, \chi, \chi^*]}{\delta\chi^*(\underline{\underline{\mathbf{R}}}\underline{\underline{\sigma}}, t)} = 0. \tag{38}$$

Variation of Eq. (37) with respect to $\Phi^*_{\underline{\underline{\mathbf{R}}}\sigma}(\underline{\underline{\mathbf{r}}}\underline{\underline{\mathbf{s}}})$ leads to

$$|\chi|^2 \left(\hat{H}_{BO} + \hat{V}^e_{\text{ext}} + \sum_\alpha \frac{-\nabla^2_\alpha}{2M_\alpha} - i\partial_t \right) \Phi_{\underline{\underline{\mathbf{R}}}\sigma}$$
$$+ \left[\chi^* \left(\sum_\alpha \frac{-\nabla^2_\alpha}{2M_\alpha} + \hat{V}^n_{\text{ext}} - i\partial_t \right) \chi \right] \Phi_{\underline{\underline{\mathbf{R}}}\sigma}$$
$$+ |\chi|^2 \left(\sum_\alpha \frac{1}{M_\alpha} (-i\nabla_\alpha \chi/\chi) \cdot (-i\nabla_\alpha \Phi_{\underline{\underline{\mathbf{R}}}\sigma}) \right) = 0.$$

Dividing the expression above by $|\chi|^2$ and rearranging yields

$$\left(\hat{H}_{BO} + \hat{V}^e_{\text{ext}} + \sum_\alpha \frac{-\nabla^2_\alpha}{2M_\alpha} - i\partial_t \right) \Phi_{\underline{\underline{\mathbf{R}}}\sigma}$$
$$+ \sum_\alpha \frac{1}{M_\alpha} (-i\nabla_\alpha \chi/\chi) \cdot (-i\nabla_\alpha \Phi_{\underline{\underline{\mathbf{R}}}\sigma})$$
$$= -\frac{\left(\sum_\alpha \frac{-\nabla^2_\alpha}{2M_\alpha} + \hat{V}^n_{\text{ext}} - i\partial_t \right) \chi}{\chi} \cdot \Phi_{\underline{\underline{\mathbf{R}}}\sigma}. \tag{39}$$

Variation of Eq. (37) with respect to χ^* yields

$$\left[\sum_{\underline{\underline{\mathbf{s}}}} \int d\underline{\underline{\mathbf{r}}} \Phi^*_{\underline{\underline{\mathbf{R}}}\sigma} \left(\hat{H}_{BO} + \hat{V}^e_{\text{ext}} + \sum_\alpha \frac{-\nabla^2_\alpha}{2M_\alpha} - i\partial_t \right) \Phi_{\underline{\underline{\mathbf{R}}}\sigma} \right] \chi$$
$$+ \left[\sum_\alpha \frac{-\nabla^2_\alpha}{2M_\alpha} + \hat{V}^n_{\text{ext}} \right] \chi + \left[\sum_\alpha \frac{1}{M_\alpha} (-i\nabla_\alpha \chi/\chi) \cdot \mathbf{A}_\alpha \right] \chi = i\partial_t \chi, \tag{40}$$

where we enforced the PNC, and defined

$$\mathbf{A}_\alpha[\Phi_{\underline{\underline{\mathbf{R}}}\sigma}] := \sum_{\underline{\underline{\mathbf{s}}}} \int d\underline{\underline{\mathbf{r}}} \Phi^*_{\underline{\underline{\mathbf{R}}}\sigma}(\underline{\underline{\mathbf{r}}}\underline{\underline{\mathbf{s}}}) (-i\nabla_\alpha \Phi_{\underline{\underline{\mathbf{R}}}\sigma}(\underline{\underline{\mathbf{r}}}\underline{\underline{\mathbf{s}}})). \tag{41}$$

This is a real-valued vector potential (see shortly). Inserting Eq. (40) on the RHS of Eq. (39) leads, after some straightforward algebra, to Eqs. (28)–(33). The product wavefunction Eq. (23), satisfying these equations, therefore represents a stationary point of the action functional (37) under the PNC Eq. (24). To complete the proof, it remains to verify that if $\Phi_{\underline{\underline{\mathbf{R}}}\sigma}(\underline{\mathbf{r}}\underline{\underline{\sigma}}, t)$ satisfies Eq. (28) and $\chi(\underline{\underline{\mathbf{R}}}\underline{\underline{\sigma}}, t)$ satisfies Eq. (29), then the product $\Phi_{\underline{\underline{\mathbf{R}}}\sigma}(\underline{\underline{\mathbf{r}}}\underline{\underline{\mathbf{s}}}, t)\chi(\underline{\underline{\mathbf{R}}}\underline{\underline{\sigma}}, t)$ is an exact solution of the TDSE. Approximate solutions of the TDSE may satisfy the stationary action principle, if variations are taken over a limited set of wavefunctions, e.g., the multi-configuration time-dependent Hartree equations[44] may be derived via the Frenkel variational principle. To dispel any possible doubts that the product form of Eq. (23) subject to Eq. (24) is general, we now verify that our solution is exact and not an approximation. Applying the product rule, $i\partial_t \Psi(\underline{\underline{\mathbf{r}}}\underline{\underline{\mathbf{s}}}, \underline{\underline{\mathbf{R}}}\underline{\underline{\sigma}}, t)$

$= \chi(\underline{\underline{\mathbf{R}}}\underline{\underline{\sigma}}, t) i\partial_t \Phi_{\underline{\underline{\mathbf{R}}}\underline{\underline{\sigma}}}(\underline{\underline{\mathbf{r}}}\underline{\underline{\mathbf{s}}}, t) + \Phi_{\underline{\underline{\mathbf{R}}}\underline{\underline{\sigma}}}(\underline{\underline{\mathbf{r}}}\underline{\underline{\mathbf{s}}}, t) i\partial_t \chi(\underline{\underline{\mathbf{R}}}\underline{\underline{\sigma}}, t)$, and inserting Eqs. (28) and (29), we obtain

$$\chi\left(i\partial_t \Phi_{\underline{\underline{\mathbf{R}}}\underline{\underline{\sigma}}}\right)$$
$$= \chi\left(\hat{H}_{BO} + \hat{V}^e_{\text{ext}}\right)\Phi_{\underline{\underline{\mathbf{R}}}\underline{\underline{\sigma}}} + \chi\sum_{\alpha}^{N_n}\frac{(-i\nabla_\alpha - \mathbf{A}_\alpha)^2}{2M_\alpha}\Phi_{\underline{\underline{\mathbf{R}}}\underline{\underline{\sigma}}}$$
$$+\chi\sum_{\alpha}^{N_n}\frac{(-i\nabla_\alpha\chi/\chi + \mathbf{A}_\alpha)\cdot(-i\nabla_\alpha - \mathbf{A}_\alpha)}{M_\alpha}\Phi_{\underline{\underline{\mathbf{R}}}\underline{\underline{\sigma}}} - \chi\epsilon\Phi_{\underline{\underline{\mathbf{R}}}\underline{\underline{\sigma}}}, \tag{42}$$

$$\Phi_{\underline{\underline{\mathbf{R}}}\underline{\underline{\sigma}}}(i\partial_t\chi) = \Phi_{\underline{\underline{\mathbf{R}}}\underline{\underline{\sigma}}}\sum_{\alpha}^{N_n}\frac{(-i\nabla_\alpha + \mathbf{A}_\alpha(\underline{\underline{\mathbf{R}}}\underline{\underline{\sigma}}, t))^2}{2M_\alpha}\chi$$
$$+\Phi_{\underline{\underline{\mathbf{R}}}\underline{\underline{\sigma}}}\hat{V}^n_{\text{ext}}\chi + \Phi_{\underline{\underline{\mathbf{R}}}\underline{\underline{\sigma}}}\epsilon\chi. \tag{43}$$

Summing Eqs. (42) and (43) leads to the TDSE for the complete system and completes the proof that the wavefunctions satisfying Eqs. (28)–(33) do solve the TDSE exactly.

Alternatively, Eqs. (28)−(33) can be obtained by replacing $\Psi(\underline{\underline{\mathbf{r}}}\underline{\underline{\mathbf{s}}}, \underline{\underline{\mathbf{R}}}\underline{\underline{\sigma}}, t)$, in the TDSE (10), by the product $\Phi_{\underline{\underline{\mathbf{R}}}\underline{\underline{\sigma}}}(\underline{\underline{\mathbf{r}}}\underline{\underline{\mathbf{s}}}, t)\chi(\underline{\underline{\mathbf{R}}}\underline{\underline{\sigma}}, t)$ and using the PNC (24). The form of electron-nuclear coupling term, Eq. (31), is the same as the static case (see Ref. 20). The exact TDPES, Eq. (32), on the other hand is not simply the expectation value of $\hat{H}_{el}$ but contains, in addition, the term $\langle\Phi_{\underline{\underline{\mathbf{R}}}\underline{\underline{\sigma}}}| - i\partial_t\Phi_{\underline{\underline{\mathbf{R}}}\underline{\underline{\sigma}}}\rangle$. The appearance of this term is essential to ensure the form invariance of the Eqs. (28) −(33) under the gauge transformation (44), that will be discussed in Sec. II B.

B. Uniqueness of the electronic and nuclear wavefunctions

We now delve a little deeper into features of our exact factorization. As briefly mentioned earlier, the factorization can be viewed in a standard probabilistic setting:[19] The square of the molecular wavefunction can be viewed as a multivariate probability distribution that can be factorized into a marginal probability of a set of variables (the nuclear coordinates) and a conditional probability of the rest of the variables (the electronic coordinates, conditionally dependent on the nuclear coordinates). In this sense, we identify $\chi(\underline{\underline{\mathbf{R}}}\underline{\underline{\sigma}}, t)$ as the nuclear wavefunction (marginal probability amplitude), and $\Phi_{\underline{\underline{\mathbf{R}}}\underline{\underline{\sigma}}}(\underline{\underline{\mathbf{r}}}\underline{\underline{\mathbf{s}}}, t)$ as the electronic wavefunction (conditional probability amplitude). An equivalent formalism is to view, instead, the nuclear wavefunction as a conditional probability amplitude depending parametrically on the electronic coordinate, i.e., $\chi_{\underline{\underline{\mathbf{r}}}\underline{\underline{\mathbf{s}}}}(\underline{\underline{\mathbf{R}}}\underline{\underline{\sigma}}, t)$, with the electronic wavefunction as the marginal probability amplitude of the electronic coordinates, i.e., $\Phi(\underline{\underline{\mathbf{r}}}\underline{\underline{\mathbf{s}}}, t)$. We choose to use the former decomposition however to later make natural connections with the BO approach. In this section, we argue why we can view the probability amplitudes $\chi(\underline{\underline{\mathbf{R}}}\underline{\underline{\sigma}}, t)$ and $\Phi_{\underline{\underline{\mathbf{R}}}\underline{\underline{\sigma}}}(\underline{\underline{\mathbf{r}}}\underline{\underline{\mathbf{s}}}, t)$ as nuclear and electronic wavefunctions, and we will assign some meaning to the terms that arise in their equations of motion.

A first question that arises is: is this decomposition unique? We answer this in Theorem 2.

Theorem 2 (a): *Equations (28)−(33) are form-invariant up to within the gauge-like transformation*

$$\tilde{\Phi}_{\underline{\underline{\mathbf{R}}}\underline{\underline{\sigma}}}(\underline{\underline{\mathbf{r}}}\underline{\underline{\mathbf{s}}}, t) := e^{i\theta(\underline{\underline{\mathbf{R}}}\underline{\underline{\sigma}}, t)}\Phi_{\underline{\underline{\mathbf{R}}}\underline{\underline{\sigma}}}(\underline{\underline{\mathbf{r}}}\underline{\underline{\mathbf{s}}}, t),$$
$$\tilde{\chi}(\underline{\underline{\mathbf{R}}}\underline{\underline{\sigma}}, t) := e^{-i\theta(\underline{\underline{\mathbf{R}}}\underline{\underline{\sigma}}, t)}\chi(\underline{\underline{\mathbf{R}}}\underline{\underline{\sigma}}, t), \tag{44}$$

$$\mathbf{A}_\alpha(\underline{\underline{\mathbf{R}}}\underline{\underline{\sigma}}, t) \to \tilde{\mathbf{A}}_\alpha(\underline{\underline{\mathbf{R}}}\underline{\underline{\sigma}}, t) = \mathbf{A}_\alpha(\underline{\underline{\mathbf{R}}}\underline{\underline{\sigma}}, t) + \nabla_\alpha\theta(\underline{\underline{\mathbf{R}}}\underline{\underline{\sigma}}, t),$$
$$\epsilon(\underline{\underline{\mathbf{R}}}\underline{\underline{\sigma}}, t) \to \tilde{\epsilon}(\underline{\underline{\mathbf{R}}}\underline{\underline{\sigma}}, t) = \epsilon(\underline{\underline{\mathbf{R}}}\underline{\underline{\sigma}}, t) + \partial_t\theta(\underline{\underline{\mathbf{R}}}\underline{\underline{\sigma}}, t). \tag{45}$$

(b) *The wavefunctions $\Phi_{\underline{\underline{\mathbf{R}}}\underline{\underline{\sigma}}}(\underline{\underline{\mathbf{r}}}\underline{\underline{\mathbf{s}}}, t)$ and $\chi(\underline{\underline{\mathbf{R}}}\underline{\underline{\sigma}}, t)$ are unique up to within the $(\underline{\underline{\mathbf{R}}}\underline{\underline{\sigma}}, t)$-dependent phase transformation, Eq. (44).*

To prove part (a), simply substitute Eqs. (44) and (45) into Eqs. (28)–(33). Part (b) is readily shown by first assuming that $\Phi_{\underline{\underline{\mathbf{R}}}\underline{\underline{\sigma}}}\chi$ and $\tilde{\Phi}_{\underline{\underline{\mathbf{R}}}\underline{\underline{\sigma}}}\tilde{\chi}$ are two different representations of the exact wave function $\Psi(\underline{\underline{\mathbf{r}}}\underline{\underline{\mathbf{s}}}, \underline{\underline{\mathbf{R}}}\underline{\underline{\sigma}}, t)$, i.e.,

$$\Psi(\underline{\underline{\mathbf{r}}}\underline{\underline{\mathbf{s}}}, \underline{\underline{\mathbf{R}}}\underline{\underline{\sigma}}, t) = \Phi_{\underline{\underline{\mathbf{R}}}\underline{\underline{\sigma}}}(\underline{\underline{\mathbf{r}}}\underline{\underline{\mathbf{s}}}, t)\chi(\underline{\underline{\mathbf{R}}}\underline{\underline{\sigma}}, t) = \tilde{\Phi}_{\underline{\underline{\mathbf{R}}}\underline{\underline{\sigma}}}(\underline{\underline{\mathbf{r}}}\underline{\underline{\mathbf{s}}}, t)\tilde{\chi}(\underline{\underline{\mathbf{R}}}\underline{\underline{\sigma}}, t).$$

Then

$$\frac{\chi}{\tilde{\chi}} = \frac{\tilde{\Phi}_{\underline{\underline{\mathbf{R}}}\underline{\underline{\sigma}}}}{\Phi_{\underline{\underline{\mathbf{R}}}\underline{\underline{\sigma}}}} =: g(\underline{\underline{\mathbf{R}}}\underline{\underline{\sigma}}, t), \tag{46}$$

and

$$|\tilde{\Phi}_{\underline{\underline{\mathbf{R}}}\underline{\underline{\sigma}}}(\underline{\underline{\mathbf{r}}}\underline{\underline{\mathbf{s}}}, t)|^2 = |g(\underline{\underline{\mathbf{R}}}\underline{\underline{\sigma}}, t)|^2|\Phi_{\underline{\underline{\mathbf{R}}}\underline{\underline{\sigma}}}(\underline{\underline{\mathbf{r}}}\underline{\underline{\mathbf{s}}}, t)|^2. \tag{47}$$

From Theorem 1, both $\tilde{\Phi}_{\underline{\underline{\mathbf{R}}}\underline{\underline{\sigma}}}(\underline{\underline{\mathbf{r}}}\underline{\underline{\mathbf{s}}}, t)$ and $\Phi_{\underline{\underline{\mathbf{R}}}\underline{\underline{\sigma}}}(\underline{\underline{\mathbf{r}}}\underline{\underline{\mathbf{s}}}, t)$ satisfy the PNC. Hence,

$$\sum_{\underline{\underline{\mathbf{s}}}}\int d\underline{\underline{\mathbf{r}}}|\tilde{\Phi}_{\underline{\underline{\mathbf{R}}}\underline{\underline{\sigma}}}(\underline{\underline{\mathbf{r}}}\underline{\underline{\mathbf{s}}}, t)|^2 = |g(\underline{\underline{\mathbf{R}}}\underline{\underline{\sigma}}, t)|^2\sum_{\underline{\underline{\mathbf{s}}}}\int d\underline{\underline{\mathbf{r}}}|\Phi_{\underline{\underline{\mathbf{R}}}\underline{\underline{\sigma}}}(\underline{\underline{\mathbf{r}}}\underline{\underline{\mathbf{s}}}, t)|^2, \tag{48}$$

and $|g(\underline{\underline{\mathbf{R}}}\underline{\underline{\sigma}}, t)|^2 = 1$. Therefore, $g(\underline{\underline{\mathbf{R}}}\underline{\underline{\sigma}}, t)$ must be equal to a purely $(\underline{\underline{\mathbf{R}}}\underline{\underline{\sigma}}, t)$-dependence phase

$$g(\underline{\underline{\mathbf{R}}}\underline{\underline{\sigma}}, t) = e^{i\theta(\underline{\underline{\mathbf{R}}}\underline{\underline{\sigma}}, t)}. \tag{49}$$

This completes the proof of Theorem 2.

The interpretation of $\Phi_{\underline{\underline{\mathbf{R}}}}$ and χ as electronic and nuclear wavefunctions follows from the following observations. The probability density of finding the nuclear configuration $\underline{\underline{\mathbf{R}}}$ at time t, $\sum_{\underline{\underline{\mathbf{s}}}}\int|\Psi(\underline{\underline{\mathbf{r}}}\underline{\underline{\mathbf{s}}}, \underline{\underline{\mathbf{R}}}\underline{\underline{\sigma}}, t)|^2 d\underline{\underline{\mathbf{r}}} = |\chi(\underline{\underline{\mathbf{R}}}\underline{\underline{\sigma}}, t)|^2$, as can readily be shown by substituting the product wavefunction Eq. (23) into the left-hand-side and using the PNC Eq. (24). Not only does $\chi(\underline{\underline{\mathbf{R}}}\underline{\underline{\sigma}}, t)$ therefore yield the nuclear (N_n-body) probability density, we shall see later in Sec. III A that it also reproduces the exact nuclear (N_n-body) current-density. The modulus-square of the electronic wavefunction, $|\Phi_{\underline{\underline{\mathbf{R}}}\underline{\underline{\sigma}}}(\underline{\underline{\mathbf{r}}}\underline{\underline{\mathbf{s}}}, t)|^2 = |\Psi(\underline{\underline{\mathbf{r}}}\underline{\underline{\mathbf{s}}}, \underline{\underline{\mathbf{R}}}\underline{\underline{\sigma}}, t)|^2/|\chi(\underline{\underline{\mathbf{R}}}\underline{\underline{\sigma}}, t)|^2$ gives the conditional probability of finding the electrons at $\underline{\underline{\mathbf{r}}}$ with spin configuration $\underline{\underline{\mathbf{s}}}$, given that the nuclear configuration is $\underline{\underline{\mathbf{R}}}\underline{\underline{\sigma}}$.

Note that, strictly speaking, the definition of the conditional probability amplitude $|\Phi_{\underline{\underline{\mathbf{R}}}\underline{\underline{\sigma}}}(\underline{\underline{\mathbf{r}}}\underline{\underline{\mathbf{s}}}, t)|^2$ via Eq. (26), only holds for non-zero marginal probabilities $|\chi(\underline{\underline{\mathbf{R}}}\underline{\underline{\sigma}}, t)|^2$. In the case the nuclear density, and the full molecular wavefunction, have a node at some $\underline{\underline{\mathbf{R}}}_0$, the electronic wavefunction would be defined by taking a limit. However, it is actually very unlikely that the nuclear density has a node.[30,31] This

can be seen by expanding the full electron-nuclear wavefunction, $\Psi(\underline{\underline{\mathbf{r}}}\underline{\underline{s}}, \underline{\underline{\mathbf{R}}}\underline{\underline{\sigma}}, t)$, in terms of the BO-electronic states, as in Eq. (17). Then, the nuclear density can be expressed as an infinite sum of non-negative terms

$$|\chi(\underline{\underline{\mathbf{R}}}\underline{\underline{\sigma}}, t)|^2 = \sum_{j=1}^{\infty} \left|\chi_j^{BO}(\underline{\underline{\mathbf{R}}}\underline{\underline{\sigma}}, t)\right|^2. \quad (50)$$

In general, it is extremely unlikely that every term in the summation becomes zero at the same nuclear configuration $\underline{\underline{\mathbf{R}}}_0\ \underline{\underline{\sigma}}_0$, unless dictated by symmetry[20] (see the end of this section for a discussion on symmetry). Symmetry-dictated nodes likely lead to a finite, well-defined, value of $|\Phi_{\underline{\underline{\mathbf{R}}}\underline{\underline{\sigma}}}(\underline{\mathbf{r}}\underline{\underline{s}}, t)|^2$ due to the linear behavior of the wavefunctions in the vicinity of these nodes.

Equations (28)–(33) determine the *exact* time-dependent molecular wavefunction, given an initial state. As written, the nuclear equation is particularly appealing as a Schrödinger equation with both scalar and vector-potential coupling terms contributing effective forces on the nuclei including any geometric phase effects. We call $\epsilon(\underline{\underline{\mathbf{R}}}\underline{\underline{\sigma}}, t)$ and $\mathbf{A}(\underline{\underline{\mathbf{R}}}\underline{\underline{\sigma}}, t)$ the *exact TDPES* and *exact time-dependent Berry connection*, respectively. These two quantities, along with the electron-nuclear coupling potential $\hat{U}_{en}^{coup}[\Phi_{\underline{\underline{\mathbf{R}}}\underline{\underline{\sigma}}}, \chi]$, mediate the coupling between the nuclear and the electronic degrees of freedom in a formally exact way. The three sections in Sec. III are each devoted to a closer study of these terms.

We conclude this section by discussing the symmetry properties of $\chi(\underline{\underline{\mathbf{R}}}\underline{\underline{\sigma}}, t)$ and $\Phi_{\underline{\underline{\mathbf{R}}}\underline{\underline{\sigma}}}(\underline{\mathbf{r}}\underline{\underline{s}}, t)$: The nuclear wavefunction $\chi(\underline{\underline{\mathbf{R}}}\underline{\underline{\sigma}}, t)$ must preserve the symmetry of the full electron-nuclear wavefunction $\Psi(\underline{\mathbf{r}}\underline{\underline{s}}, \underline{\underline{\mathbf{R}}}\underline{\underline{\sigma}}, t)$ with respect to exchange of identical nuclei. This constrains the allowed gauge transformation (44)–(45). The electronic wavefunction $\Phi_{\underline{\underline{\mathbf{R}}}\underline{\underline{\sigma}}}(\underline{\mathbf{r}}\underline{\underline{s}}, t) = \Psi(\underline{\mathbf{r}}\underline{\underline{s}}, \underline{\underline{\mathbf{R}}}\underline{\underline{\sigma}}, t)/\chi(\underline{\underline{\mathbf{R}}}\underline{\underline{\sigma}}, t)$ is invariant under any nuclear permutation because any fermionic sign cancels out between the full molecular wavefunction and the nuclear wavefunction.

In the rest of the paper, we drop the spin indices $\underline{\underline{\sigma}}$ and $\underline{\underline{s}}$ for notational simplicity.

C. Simple illustration: The H atom in an electric field

The example of the hydrogen atom in an electric field provides a simple demonstration of our formalism. The Hamiltonian is

$$H = -\frac{1}{2M}\nabla_R^2 - \frac{1}{2}\nabla_r^2 - \frac{1}{|\mathbf{R}-\mathbf{r}|} + (\mathbf{r}-\mathbf{R})\cdot\mathbf{E}(t), \quad (51)$$

where $\mathbf{r}$ and $\mathbf{R}$ are the electron and proton coordinates, respectively, $\mathbf{E(t)}$ is the applied electric field, and M is the proton mass. The exact solution is known: in terms of the center of mass and relative coordinates, $\mathbf{R}_{\mathrm{CM}} = (\mathbf{r} + M\mathbf{R})/(M+1)$, $\mathbf{u} = \mathbf{r} - \mathbf{R}$, the problem is separable, and we have

$$\Psi(\mathbf{R}_{\mathrm{CM}}, \mathbf{u}, t) = e^{i(\mathbf{K}\cdot\mathbf{R}_{\mathrm{CM}} - \frac{K^2}{2(M+1)}t)}\phi(\mathbf{u}, t), \quad (52)$$

where $\phi(\mathbf{u}, t)$ satisfies the following equation:

$$\left(-\frac{\nabla_u^2}{2\mu} - \frac{1}{u} + \mathbf{u}\cdot\mathbf{E}(t)\right)\phi(\mathbf{u}, t) = i\,\partial_t\phi(\mathbf{u}, t), \quad (53)$$

and $\mu = M/(M+1)$ is the reduced mass. The full wavefunction, Eq. (52), represents free-particle plane-wave motion in the center of mass coordinate, with $\mathbf{K}$ representing the total momentum of the system. The form of Eq. (52) suggests one possible factorization for Eqs. (23) and (24) as

$$\chi(\mathbf{R}, t) = e^{i(\frac{-K^2 t}{2(M+1)} + \frac{M}{(M+1)}\mathbf{K}\cdot\mathbf{R})},$$
$$\Phi_{\mathbf{R}}(\mathbf{r}, t) = e^{i\mathbf{K}\cdot\mathbf{r}/(M+1)}\phi(\mathbf{r}-\mathbf{R}, t), \quad (54)$$

with the exact Berry potential and TDPES given by

$$\mathbf{A}(\mathbf{R}, t) = -i\int \phi^*(\mathbf{r}-\mathbf{R}, t)\nabla_{\mathbf{R}}\phi(\mathbf{r}-\mathbf{R}, t)d\mathbf{r} = 0, \quad (55)$$

$$\epsilon(\mathbf{R}, t) = \frac{K^2}{2(M+1)} + \mathbf{R}\cdot\mathbf{E}(t). \quad (56)$$

The vector potential, Eq. (55), is zero in the gauge implicit in our choice for Eq. (54). This is easily confirmed by inserting Eq. (54) in the nuclear equation (29), which reads for our problem

$$\left(\frac{1}{M}(-i\nabla + \mathbf{A})^2 - \mathbf{R}\cdot\mathbf{E}(t) + \epsilon(\mathbf{R}, t)\right)\chi(\mathbf{R}, t) = i\,\partial_t\chi(\mathbf{R}, t). \quad (57)$$

Equations (56) and (57) show that, in this case, the role of the TDPES is to cancel out the external laser field in the nuclear equation, which is exactly as it should be. Only by this cancellation, the nuclear motion can be a plane wave.

III. THE EXACT ELECTRON-NUCLEAR COUPLING TERMS

We now take a closer look at each of the three terms $\mathbf{A}(\underline{\underline{\mathbf{R}}}\underline{\underline{\sigma}}, t)$, $\epsilon(\underline{\underline{\mathbf{R}}}\underline{\underline{\sigma}}, t)$, and $\hat{U}_{en}^{coup}[\Phi_{\underline{\underline{\mathbf{R}}}\underline{\underline{\sigma}}}, \chi]$, that mediate the coupling between electron and nuclear dynamics exactly. In these three terms, all of the non-adiabatic coupling effects of the Born-Oppenheimer expansion are effectively contained.

A. The time-dependent Berry connection

Equations (28)–(33) demonstrate that a Berry connection indeed appears in the exact treatment of coupled electron-ion dynamics, a question which was raised in the Introduction. In this section, we point out some properties of this object to help us understand what it represents.

First, we show that the vector potential $\mathbf{A}_\alpha$ is real. Taking the gradient with respect to nuclear coordinates of the PNC (Eq. (24)), yields

$$0 = \nabla_\alpha \int d\underline{\underline{\mathbf{r}}}\Phi_{\underline{\underline{\mathbf{R}}}}^*(\underline{\underline{\mathbf{r}}})\Phi_{\underline{\underline{\mathbf{R}}}}(\underline{\underline{\mathbf{r}}}),$$
$$= 2\mathrm{Re}\int d\underline{\underline{\mathbf{r}}}\Phi_{\underline{\underline{\mathbf{R}}}}^*(\underline{\underline{\mathbf{r}}})\nabla_\alpha\Phi_{\underline{\underline{\mathbf{R}}}}(\underline{\underline{\mathbf{r}}}), \quad (58)$$

(using the product rule). Comparing with the definition Eq. (33), we readily conclude $\mathbf{A}_\alpha$ is real.

Second, we insert Eqs. (25) and (26) into Eq. (33) to reveal the following expression for the vector potential:

$$\mathbf{A}_\alpha(\underline{\underline{\mathbf{R}}},t)=\frac{Im\,\langle\Psi(t)|\,\nabla_\alpha\Psi(t)\rangle_{\underline{\mathbf{r}}}}{|\chi(\underline{\underline{\mathbf{R}}},t)|^2}-\nabla_\alpha S(\underline{\underline{\mathbf{R}}},t). \tag{59}$$

This shows that the vector potential is the difference of paramagnetic nuclear velocity fields derived from the full and nuclear wavefunctions. In fact, since $Im\,\langle\Psi(t)|\,\nabla_\alpha\Psi(t)\rangle_{\underline{\mathbf{r}}}$ is the true nuclear (many-body) current density, Eq. (59) implies that the gauge-invariant current density, $Im(\chi^*\nabla_\alpha\chi)+|\chi|^2\mathbf{A}_\alpha$, that follows from the nuclear Hamiltonian in Eq. (29) does indeed reproduce the exact nuclear current density.[32] As discussed in Sec. II, the solution $\chi(\underline{\underline{\mathbf{R}}},t)$ of Eq. (28) yields a proper nuclear many-body wavefunction: Its absolute-value squared gives the exact nuclear (N_n-body) density while its phase yields the correct nuclear (N_n-body) current density. (The nuclear kinetic energy evaluated from $\chi(\underline{\underline{\mathbf{R}}},t)$ does not equal the nuclear kinetic energy evaluated from the full molecular wavefunction, and their difference is determined by U_{en}^{coup}, as will be discussed in Sec. III C).

Another interesting aspect of expression (59) is that it can help to shed light on the question of whether the exact Berry potential produces a real effect or whether it can actually be gauged away by a suitable choice of $\theta(\underline{\underline{\mathbf{R}}},t)$ in Eqs. (44)–(45). Provided the phase $S(\underline{\underline{\mathbf{R}}},t)$ is spatially smooth, the last term on the right-hand-side of Eq. (59) can be gauged away so any true Berry connection (that cannot be gauged away) must come from the first term. In the conventional analyses of conical intersections, the phase may not be smooth: for example, in the Herzberg and Longuet-Higgens model,[26,45] the two (single-valued) nuclear wavefunctions associated with a two-state conical intersection between traditional BO surfaces, each have a phase $S=\pm\phi/2$, undefined at the origin. This has a singular gradient, yielding a delta-function at the origin in the curl of the vector potential, thus contributing a non-zero Berry phase. Whether a similar effect occurs for the exact time-dependent nuclear wavefunction remains to be explored. When the exact $\Psi(t)$ is real-valued (e.g., for a non-current-carrying ground state) then the first term on the right-hand-side of Eq. (59) vanishes and hence gives a vanishing contribution to the exact Berry connection. Whether, and under which conditions, the full Berry connection (59) can be gauged away remains an open question at this point.

Finally, it is also instructive to express the vector potential in terms of the BO electronic basis states of Sec. I C. We first expand the electronic wavefunction

$$\Phi_{\underline{\underline{\mathbf{R}}}}(\underline{\mathbf{r}},t)=\sum_{j=1}^{\infty}C_j(\underline{\underline{\mathbf{R}}},t)\phi_{\underline{\underline{\mathbf{R}}}}^j(\underline{\mathbf{r}}), \tag{60}$$

where orthonormality of the $\phi_{\underline{\underline{\mathbf{R}}}}^j$ (Eq. (16)) means

$$C_j(\underline{\underline{\mathbf{R}}},t)=\int d\underline{\mathbf{r}}\,\phi_{\underline{\underline{\mathbf{R}}}}^{j*}(\underline{\mathbf{r}})\Phi_{\underline{\underline{\mathbf{R}}}}(\underline{\mathbf{r}},t). \tag{61}$$

The PNC condition becomes

$$\sum_{j=1}^{\infty}|C_j(\underline{\underline{\mathbf{R}}},t)|^2=1. \tag{62}$$

Inserting Eq. (60) into Eq. (33), and noting the definition of the non-adiabatic derivative couplings of Eq. (22), we obtain

$$\mathbf{A}_\alpha(\underline{\underline{\mathbf{R}}},t)=\sum_{j=1}^{\infty}\Bigg(-iC_j^*(\underline{\underline{\mathbf{R}}},t)\nabla_\alpha C_j(\underline{\underline{\mathbf{R}}},t)+|C_j(\underline{\underline{\mathbf{R}}},t)|^2\mathcal{F}_{jj,\alpha}^{BO}(\underline{\underline{\mathbf{R}}})+\sum_{l\neq j}^{\infty}C_l^*(\underline{\underline{\mathbf{R}}},t)C_j(\underline{\underline{\mathbf{R}}},t)\mathcal{F}_{lj,\alpha}^{BO}(\underline{\underline{\mathbf{R}}})\Bigg). \tag{63}$$

The exact Berry potential is thereby expressed as a linear combination of the diagonal and off-diagonal BO derivative couplings. Any gauge-invariant part of the Berry connection, that would give rise to a non-zero Berry phase, arises from the part of Eq. (63) that has a non-zero curl. In the case of a real-valued electronic wavefunction, each of the three terms of Eq. (63) vanishes independently giving rise to a zero vector potential.

B. The time-dependent potential energy surface

The time-dependent potential energy surface $\epsilon(\underline{\underline{\mathbf{R}}},t)$ of Eq. (32) provides an exact time-dependent generalization of the adiabatic BO potential energy surface. As such, it should prove to be a powerful interpretive tool for general time-dependent problems. This will be explored in Sec. IV. We now begin by analyzing the expression Eq. (32) in a little more detail.

First, consider the expectation value of the electron-nuclear coupling term of Eq. (31), $\langle\Phi_{\underline{\underline{\mathbf{R}}}}|\hat{U}_{en}^{coup}|\Phi_{\underline{\underline{\mathbf{R}}}}\rangle$ that appears in the TDPES. Only the first term of Eq. (31) contributes to the expectation value: the second term goes to zero, due to the very last parenthesis, $\langle\Phi_{\underline{\underline{\mathbf{R}}}}|-i\nabla_\alpha-\mathbf{A}_\alpha(\underline{\underline{\mathbf{R}}},t)|\Phi_{\underline{\underline{\mathbf{R}}}}\rangle$, which vanishes due to the definition of the vector potential. So we have

$$\begin{aligned}\epsilon(\underline{\underline{\mathbf{R}}},t)&=\Bigg(\langle\Phi_{\underline{\underline{\mathbf{R}}}}|\hat{H}_{BO}+\hat{V}_{\rm ext}^e(\underline{\mathbf{r}},t)|\Phi_{\underline{\underline{\mathbf{R}}}}\rangle_{\underline{\mathbf{r}}}-i\langle\Phi_{\underline{\underline{\mathbf{R}}}}|\partial_t\Phi_{\underline{\underline{\mathbf{R}}}}\rangle_{\underline{\mathbf{r}}}\\&\quad+\sum_\alpha\frac{\langle\Phi_{\underline{\underline{\mathbf{R}}}}|(-i\nabla_\alpha-\mathbf{A}_\alpha(\underline{\underline{\mathbf{R}}},t))^2|\Phi_{\underline{\underline{\mathbf{R}}}}\rangle_{\underline{\mathbf{r}}}}{2M_\alpha}\Bigg),\\&=\Bigg(\langle\Phi_{\underline{\underline{\mathbf{R}}}}|\hat{H}_{BO}+\hat{V}_{\rm ext}^e(\underline{\mathbf{r}},t)|\Phi_{\underline{\underline{\mathbf{R}}}}\rangle_{\underline{\mathbf{r}}}-i\langle\Phi_{\underline{\underline{\mathbf{R}}}}|\partial_t\Phi_{\underline{\underline{\mathbf{R}}}}\rangle_{\underline{\mathbf{r}}}\\&\quad+\sum_\alpha\frac{\langle\nabla_\alpha\Phi_{\underline{\underline{\mathbf{R}}}}|\nabla_\alpha\Phi_{\underline{\underline{\mathbf{R}}}}\rangle_{\underline{\mathbf{r}}}}{2M_\alpha}\Bigg)-\sum_\alpha\frac{\mathbf{A}_\alpha^2(\underline{\underline{\mathbf{R}}},t)}{2M_\alpha},\end{aligned} \tag{64}$$

where the second line results from expanding the square in the first, and making use of the definition of the vector potential.

As we did for the vector potential, we now provide an expression for the TDPES as an expansion over BO states. Inserting Eq. (60) into Eq. (64) and performing a little straightforward algebra, we obtain

$$\epsilon(\underline{\underline{\mathbf{R}}},t)=\sum_j|C_j(\underline{\underline{\mathbf{R}}},t)|^2V^j_{BO}(\underline{\underline{\mathbf{R}}})+\sum_{jl}C^*_j(\underline{\underline{\mathbf{R}}},t)C_l(\underline{\underline{\mathbf{R}}},t)\langle\phi^j_{\underline{\underline{\mathbf{R}}}}|\hat{V}^e_{\rm ext}(\underline{\mathbf{r}},t)|\phi^l_{\underline{\underline{\mathbf{R}}}}\rangle_{\underline{\mathbf{r}}}-\sum_j iC^*_j(\underline{\underline{\mathbf{R}}},t)\partial_tC_j(\underline{\underline{\mathbf{R}}},t)$$
$$+\sum_\alpha\frac{1}{2M_\alpha}\left(\sum_j|\nabla_\alpha C_j|^2+\sum_{jl}C^*_jC_l\left(i\nabla_\alpha\cdot\mathcal{F}^{BO}_{jl,\alpha}-\mathcal{G}^{BO}_{jl,\alpha}\right)-2\sum_{jl}\mathrm{Im}\left(C_l\nabla_\alpha C^*_j\mathcal{F}^{BO}_{jl,\alpha}\right)-\mathbf{A}^2_\alpha(\underline{\underline{\mathbf{R}}},t)\right) \quad (65)$$

(the expansion of the last term $\mathbf{A}^2_\alpha$ may be obtained from Eq. (63)). Notice that all the BO surfaces, as well as non-adiabatic couplings, are contained in the the exact TDPES.

C. Electron-nuclear correlation

The TDPES and Berry connection discussed in Secs. III A and III B directly determine the evolution of the nuclear wavefunction (Eq. (29)), containing the effect of coupling to the electrons in an exact way. The electron-nuclear coupling term $\hat{U}^{coup}_{en}$ enters the nuclear equation indirectly via its role in determining $\Phi_{\underline{\underline{\mathbf{R}}}}$ through Eqs. (28) and (30). Equation (31) expresses $\hat{U}^{coup}_{en}$ as a functional of the electronic and nuclear wavefunctions, and now we shall derive another expression for it that shows that it measures the difference between the nuclear kinetic energy evaluated from the full wavefunction and that evaluated on the nuclear wavefunction. We isolate the term involving $\hat{U}^{coup}_{en}$ in Eq. (28), and insert $\Phi_{\underline{\underline{\mathbf{R}}}}=\Psi/\chi$. This leads to

$$\frac{\hat{U}^{coup}_{en}\Phi_{\underline{\underline{\mathbf{R}}}}}{\Phi_{\underline{\underline{\mathbf{R}}}}}=\frac{i\,\partial_t\Psi}{\Psi}-\frac{i\,\partial_t\chi}{\chi}-\frac{\hat{H}_{BO}\Phi_{\underline{\underline{\mathbf{R}}}}}{\Phi_{\underline{\underline{\mathbf{R}}}}}-\hat{V}^e_{\rm ext}+\epsilon(\underline{\underline{\mathbf{R}}},t). \quad (66)$$

Next we insert in Eq. (66) the TDSE (10) and Eq. (29), satisfied by Ψ and χ to obtain

$$\frac{\hat{U}^{coup}_{en}[\Phi_{\underline{\underline{\mathbf{R}}}},\chi]\Phi_{\underline{\underline{\mathbf{R}}}}(\underline{\mathbf{r}},t)}{\Phi_{\underline{\underline{\mathbf{R}}}}(\underline{\mathbf{r}},t)}=\frac{\hat{T}_n\Psi}{\Psi}-\frac{\hat{\tilde{T}}_n\chi}{\chi}, \quad (67)$$

where

$$\hat{\tilde{T}}_n=\sum_{\alpha=1}^{N_n}\frac{1}{2M_\alpha}(-i\nabla_\alpha+\mathbf{A}_\alpha(\underline{\underline{\mathbf{R}}},t))^2. \quad (68)$$

Multiplying Eq. (67) by $|\Phi_{\underline{\underline{\mathbf{R}}}}|^2|\chi|^2$ and integrating over all coordinates leads to

$$\langle\Psi|\hat{T}_n|\Psi\rangle_{\underline{\mathbf{r}},\underline{\underline{\mathbf{R}}}}-\langle\chi|\hat{\tilde{T}}_n|\chi\rangle_{\underline{\underline{\mathbf{R}}}}=\int d\underline{\underline{\mathbf{R}}}|\chi(\underline{\underline{\mathbf{R}}},t)|^2\langle\Phi_{\underline{\underline{\mathbf{R}}}}|\hat{U}^{coup}_{en}|\Phi_{\underline{\underline{\mathbf{R}}}}\rangle_{\underline{\mathbf{r}}}. \quad (69)$$

This means the nuclear kinetic energy evaluated from the full molecular wavefunction, and that evaluated via the expectation value of the nuclear kinetic energy operator in Eq. (29) on the nuclear wavefunction are not equal: their difference is given by the nuclear-density-weighted integral of the electron-nuclear coupling potential.

IV. MODEL OF H_2^+ IN A LASER FIELD

In this section, we illustrate the usefulness of the TDPES using a simple, numerically exactly solvable model: the H_2^+ molecular ion subject to a linearly polarized laser field. By restricting the motion of the nuclei and the electron to the direction of the polarization axis of the laser field, the problem can be modeled with a 1D Hamiltonian featuring "soft-Coulomb" interactions[33–37]

$$\hat{H}(t)=-\frac{1}{M}\frac{\partial^2}{\partial R^2}-\frac{1}{2\mu_e}\frac{\partial^2}{\partial x^2}+\frac{1}{\sqrt{0.03+R^2}}+\hat{V}_l(x,t)$$
$$-\frac{1}{\sqrt{1+(x-R/2)^2}}-\frac{1}{\sqrt{1+(x+R/2)^2}}, \quad (70)$$

where R and x are the internuclear distance and the electronic coordinate as measured from the nuclear center-of-mass, respectively, and the electronic reduced mass is given by $\mu_e=(2M)/(2M+1)$, M being the proton mass. The laser field is represented by $\hat{V}_l(x,t)=q_exE(t)$, where $E(t)$ denotes the electric field amplitude and the reduced charge $q_e=(2M+2)/(2M+1)$. One-dimensional soft-Coulomb atoms and molecules have proven extremely useful in the study of strong-field dynamics since they allow numerically accurate solutions to problems involving correlated electron dynamics as well as correlated electron-nuclear dynamics that would be computationally far more demanding for the full three-dimensional atoms and molecules, while capturing the essential physics of the latter, e.g., multi-photon ionization, above-threshold ionization and dissociation, enhanced ionization, non-sequential double-ionization, high-harmonic generation, and non-BO effects (e.g., Refs. 7 and 35–41). We study the dynamics of the model H_2^+ system under a $\lambda=228$ nm (5.4 eV) UV-laser pulse, which is represented by

$$E(t)=E_0f(t)\sin(\omega t), \quad (71)$$

with two peak intensities, $I_1=|E_0|^2=10^{14}\,\mathrm{W/cm^2}$ and $I_2=|E_0|^2=2.5\times10^{13}\,\mathrm{W/cm^2}$. With this frequency, an energy that is about twice as much as the dissociation energy of the model molecule (2.8782 eV) is achieved, so dissociation is expected. The envelope function $f(t)$ is chosen such that the field is linearly ramped from zero to its maximum strength at $t=T_{ramp}$ and thereafter held constant (Fig. 1)

$$f(t)=\begin{cases}t/T_{ramp} & 0<t<T_{ramp}\\ 1 & T_{ramp}<t<T_{tot}\end{cases}. \quad (72)$$

The rise-time was chosen as $T_{ramp}=10\tau$ while the total simulation time was $T_{tot}=25\tau$, where $\tau=\frac{2\pi}{\omega}$ denotes the optical cycle.

The same system and parameters were studied in Ref. 37 where the importance of electron-nuclear correlation was highlighted: a two-configuration correlated ansatz for the time-dependent electron-nuclear wavefunction was able

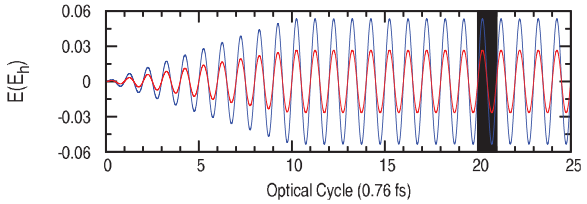

FIG. 1. $\lambda = 228$ nm laser field, represented by $E(t) = E_0 f(t)\sin(\omega t)$, for two peak intensities, $I_1 = |E_0|^2 = 10^{14}$ W/cm^2 and $I_2 = |E_0|^2 = 2.5 \times 10^{13}$ W/cm^2. The envelope function $f(t)$ is chosen such that the field is linearly ramped from zero to its maximum strength at $t = 7.6$ fs and thereafter held constant. The highlighted area represents the optical cycle that will be focussed on in later graphs.

to describe photodissociation processes in many cases, while a simple uncorrelated Hartree product of an electronic and a nuclear wavefunction almost always failed. In the present work, we analyse the dynamics via the numerically exact TDPES, finding it very useful in understanding and interpreting the motion. We note that the laser-field does not couple directly to the nuclear relative coordinate R, but only indirectly via the TDPES.

Starting from the exact ground-state as initial condition, we propagate the TDSE numerically, using the second-order split-operator method,[42] to obtain the full molecular wavefunction $\Psi(x, R, t)$. As there is only one nuclear degree of freedom (after separating off the center-of-mass motion), we can fix the gauge in Eqs. (44)–(45) such that the vector potential (59) vanishes identically. For one-dimensional problems, this is always possible with the choice

$$\frac{d}{dR}S(R,t) = \frac{Im\int dx \Psi^*(x,R,t)\frac{d\Psi(x,R,t)}{dR}}{|\chi(R,t)|^2}. \qquad (73)$$

So we can calculate $S(R, t)$, the phase of the nuclear wavefunction, as well as $|\chi(R, t)|^2$, the nuclear density, from the computed exact time-dependent molecular wavefunction. Being equipped with the nuclear wave-function, $\chi(R, t)$ $(= |\chi(R, t)|e^{iS(R,t)})$, we then compute the TDPES by inverting the nuclear equation of motion (29).

We will compare the exact dynamics with the following three approximations: (i) the usual Ehrenfest approximation, where the nuclei are treated via classical dynamics, evolving under the force $-\nabla V_{Ehr} = -\nabla_{\underline{\mathbf{R}}} W_{nn}(\underline{\mathbf{R}}) - \int d\underline{\mathbf{r}} n(\mathbf{r}, t)\nabla_{\underline{\mathbf{R}}} W_{en}(\underline{\mathbf{r}}, \underline{\mathbf{R}})$, with $n(\mathbf{r}, t)$ being the one-body electron density, (ii) the "exact-Ehrenfest" approximation, which substitutes the exact TDPES for the Ehrenfest potential V_{Ehr} in the usual Ehrenfest approach, and (iii) an uncorrelated approach, the time-dependent Hartree (self-consistent field) approximation, $\Psi_H(\underline{\mathbf{r}}, \underline{\mathbf{R}}, t) = \phi(\underline{\mathbf{r}}, t)\chi(\underline{\mathbf{R}}, t)$, where the electronic part does not depend on $\underline{\mathbf{R}}$ at all. This includes a quantum treatment of the nuclei, but no electron-nuclear correlation.

A. High intensity: $I_1 = 10^{14}$ W/cm^2

The exact TDPES, along with the corresponding nuclear density, $|\chi(R, t)|^2$, are plotted in Fig. 2 at six snapshots of time. The initial TDPES lies practically on top of the ground-state BO surface, plotted in all the snapshots for comparison.

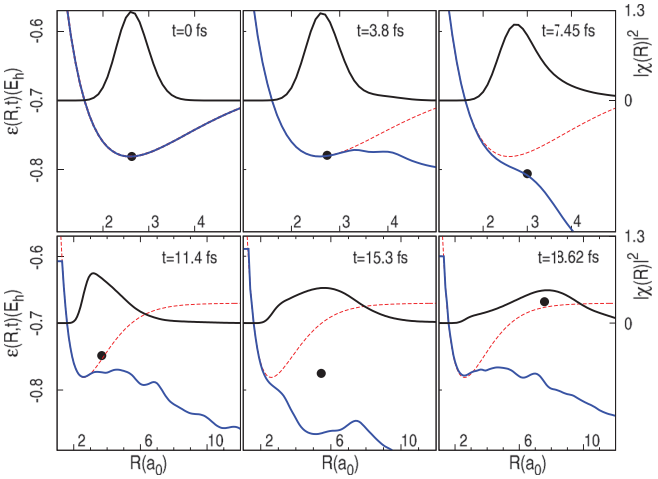

FIG. 2. Snapshots of the TDPES (blue solid lines) and nuclear density (black solid lines) at times indicated, for the H_2^+ molecule subject to the laser-field with the peak intensity $I_1 = 10^{14}$ W/cm^2. The solid circles indicate the position and energy of the classical particle in the exact-Ehrenfest calculation. For reference, the ground-state BO surface (red dashed lines) is shown.

The dissociation of the molecule is dramatically reflected in the exact TDPES, whose well flattens out, causing the nuclear density to spill to larger separations. Importantly, the tail of the TDPES alternately falls sharply and returns in correspondence with the field, letting the density out; the TDPES is the only potential acting on the nuclear system and transfers energy from the accelerated electron to the nuclei.

In Fig. 3, we focus on six equally-spaced time snapshots during the optical cycle shaded in Fig. 1. The lower panel shows the TDPES, with its characteristic oscillations, along with the nuclear density as a function of the internuclear coordinate, $|\chi(R, t)|^2$. The upper panel shows a color map of the conditional electronic probability density,

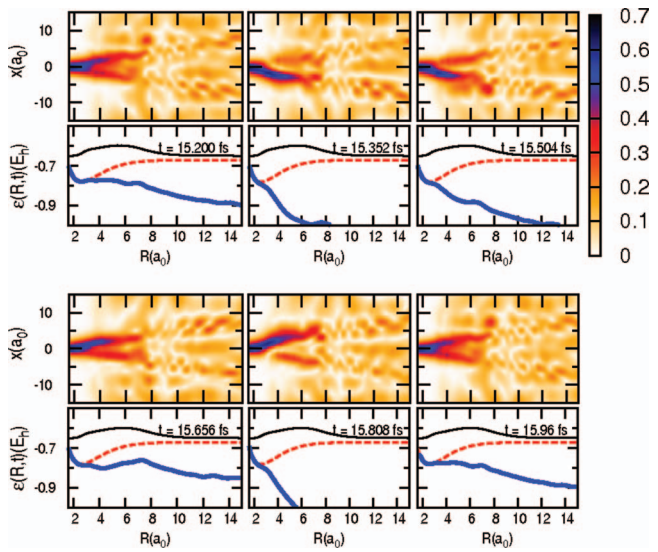

FIG. 3. Snapshots of the TDPES (blue lines), nuclear density (black), and the electronic conditional-density (color map) at times indicated during an optical cycle, for the H_2^+ molecule subject to the laser-field with the peak intensity $I_1 = 10^{14}$ W/cm^2. For reference, the ground-state BO surface is shown as the red line.

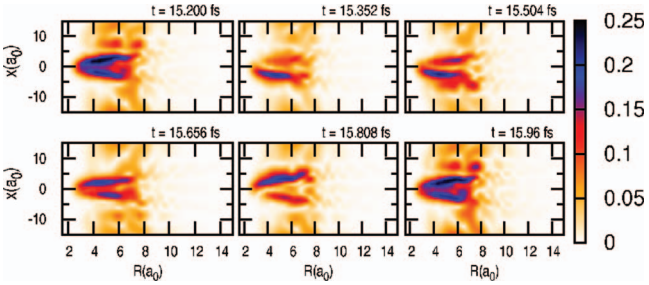

FIG. 4. Snapshots of the total electron-nuclear density at times indicated during an optical cycle, for the H_2^+ molecule subject to the laser-field with the peak intensity $I_1 = 10^{14}$ W/cm^2.

$|\Phi_R(x, t)|^2$, i.e., the probability of finding an electron at x at a fixed nuclear separation R. While at small internuclear distances (around and below the equilibrium separation), the electron remains localized in the middle between the two nuclei, at larger separations one clearly sees the preferential localization of the electron density near the two nuclei, i.e., on one side or the other. At even larger separations, we see streaks of ionizing electron density in both directions. For the full story, we must multiply the conditional probability density of the upper panels with the nuclear density shown in the lower panel, to obtain the total electron-nuclear density; this is shown in Figure 4, indicating the probability of finding, at the time indicated, an electron at position x and the nuclear separation R.

The top left-hand panel of Fig. 5 shows the expectation value of the internuclear distance

$$\langle \hat{R} \rangle = \langle \Psi(t) | \hat{R} | \Psi(t) \rangle, \tag{74}$$

along with the results from the three approximate methods described earlier. The lower left-hand panel shows the ionization probabilities. In principle, the latter requires projections of the full wavefunction on all continuum states, which, in practice, are difficult to calculate. Alternatively, we use a geometrical concept,[47] according to which the total ionization probabilities can be obtained from

$$P_{ion}(t) = 1 - \int_{box_e} dx \left(\int dR |\Psi(t)|^2 \right). \tag{75}$$

The electrons leaving the "electronic analyzing box" (box_e) are thereby identified with ionized electrons. The ionization box here was chosen to be $|x| \leq 10$. The internuclear distance together with the ionization probability support a Coulomb-explosion interpretation of the dissociation: first, the system begins to ionize, then the nuclei begin to rapidly move apart under their mutual Coulomb repulsion increasingly sensed due to weaker screening by the reduced electron density. Turning now to the approximations, we observe that all the methods yield dissociation and some ionization. The expectation value of the internuclear distance in Fig. 5, demonstrates that among all the approximate calculations employed here, the exact-Ehrenfest is most accurate. Referring back to Figure 2: the solid circles indicate the classical nuclear position and energy of a particle driven by the exact-Ehrenfest force. One can see that it rapidly picks up kinetic energy above the TDPES, supporting the fact that the nuclear dissociation mechanism is an essentially classical one in this case. The exact-Ehrenfest calculation even does better than TD-Hartree, which treats the protons quantum mechanically, thus showing the overarching importance of electron-nuclear correlation in this case.

In fact, the Hartree description is worse than it may seem from just looking at the internuclear separation in Fig. 5. In Figure 6, we plot the time-dependent Hartree potential energy surface and Hartree nuclear-density. Both are dramatically different from the exact TDPES and exact nuclear density of Figure 2. At the initial time, the Hartree potential is reasonably good near equilibrium but poor at large separations:[37] this is a consequence of the conditional electron probability being independent of the nuclear coordinate, and therefore only yielding a realistic result where the energy is optimized, which is at equilibrium separation. As time evolves the minimum of the Hartree surface moves out and

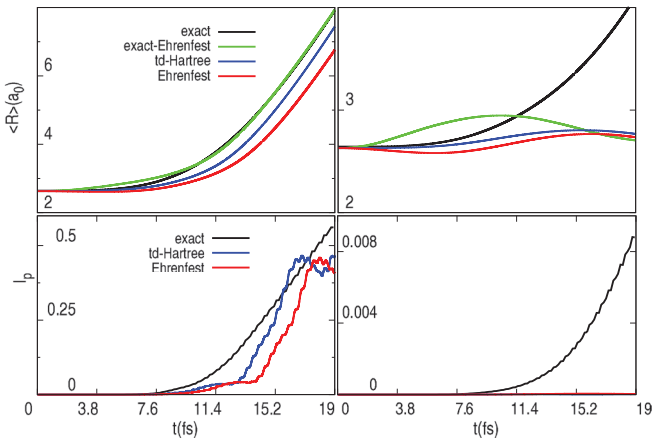

FIG. 5. Dissociation and ionization for intensity I_1 (left) and I_2 (right). Top panels: the internuclear separation $\langle R \rangle(t)$. Lower panels: the ionization probability.

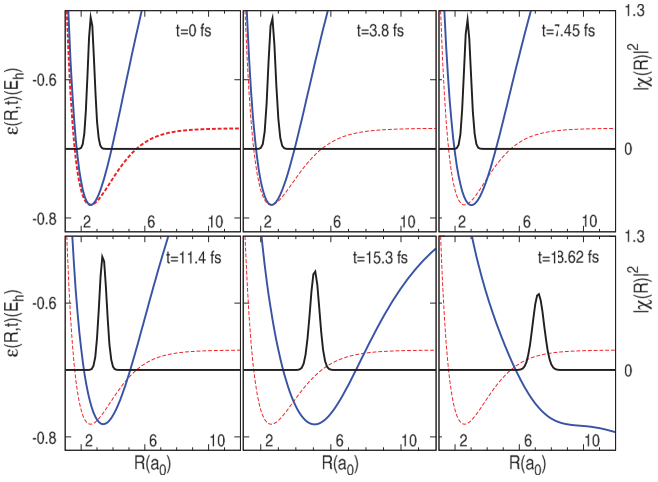

FIG. 6. Snapshots of the time-dependent Hartree nuclear-potential (blue lines) and nuclear density (black) at times indicated, for the H_2^+ molecule subject to the laser-field with the peak intensity $I_1 = 10^{14}$ W/cm^2. For reference, the ground-state BO surface is shown as the red line.

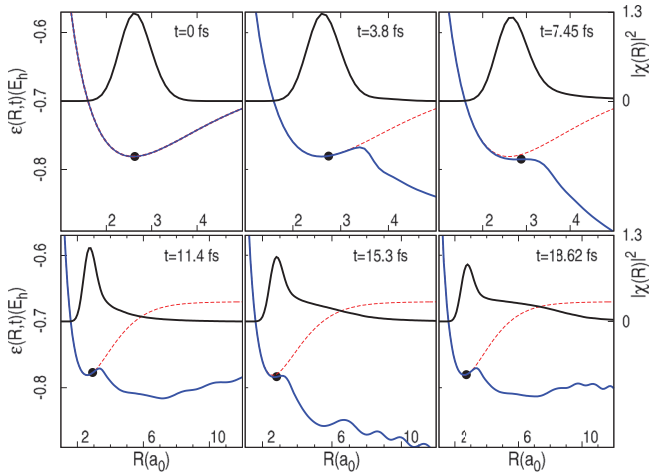

FIG. 7. Snapshots of the TDPES (blue) and nuclear density (black) at times indicated, for the H_2^+ molecule subject to the laser-field with the peak intensity $I_2 = 2.5 \times 10^{13}$ W/cm^2. The solid circles indicate the position and energy of the classical particle in the exact-Ehrenfest calculation. For reference, the ground-state BO surface (dashed red) is shown.

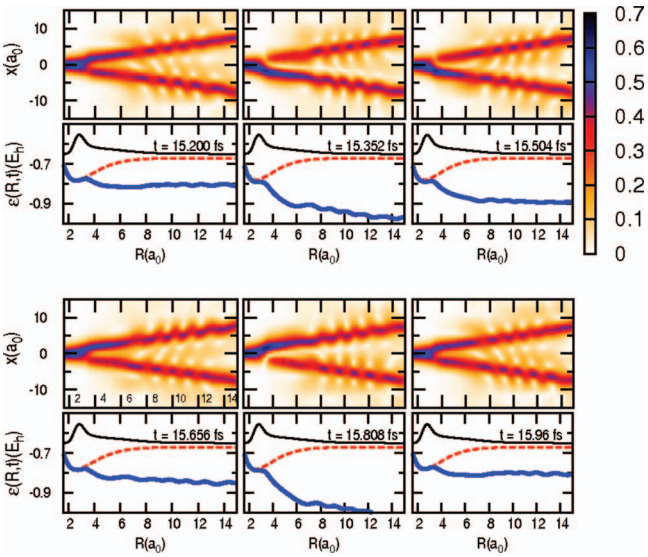

FIG. 8. Snapshots of the TDPES (blue lines), nuclear density (black), and the electronic conditional-density (color map) at times indicated during an optical cycle, for the H_2^+ molecule subject to the laser-field with the peak intensity $I_2 = 2.5 \times 10^{13}$ W/cm^2 . For reference, the ground-state BO surface is shown as the dashed red line.

begins to widen, cradling the nuclear density, which more or less retains its Gaussian shape, unlike the exact density; only at larger times does the surface open out.

B. Lower intensity: $I_2 = 2.5 \times 10^{13}$ W/cm^2

We now consider the dynamics under a field of weaker intensity. Figure 7 plots the TDPES, whose tail displays similar oscillations as in the higher intensity case. The nuclear density appears to leak out to larger separations, although more slowly than in the previous case; indeed from the right panels in Fig. 5, we see that the exact calculation leads to dissociation. However, Fig. 5 (upper right panel) also shows that none of the approximations dissociates, in contrast to the previous case. The Hartree and Ehrenfest methods also show negligible ionization, compared to the exact case; but even in the exact case, the ionization probability is very small, indicating a different mechanism of dissociation than in the stronger field case. It may be at first surprising that the exact-Ehrenfest calculation does not dissociate the molecule, given that it is based on the exact TDPES, however an examination of classical dynamics in the TDPES of Fig. 2 can explain what is happening. The solid dot in Fig. 2 indicates the classical position and energy, and we see that it is always trapped inside a well in the TDPES that remains at all times. This suggests that tunneling is the leading mechanism for the dissociation: a classical particle can only oscillate inside the well, while a quantum particle may tunnel out, as indeed reflected in Fig. 5. Although the tail has similar oscillations as for I_1, this does not lead to the dissociation of classical nuclei due to the barrier; the TDPES in this case transfers the field energy to the nuclei via tunneling. Although the exact-Ehrenfest calculation shows a larger amplitude of oscillation than the others, it ultimately cannot tunnel through the barrier.

As in the previous case, we plot in the top panels of Fig. 8 the electronic conditional density $|\Phi_R(x, t)|^2$ over one optical cycle, while the lower panels illustrate again the opening and closing of the TDPES as the field oscillates. Like in the previous case, for small R near equilibrium, the electron density is localized in between the nuclei, while for larger R, there is some polarization towards one side or the other. To get the full picture, one must multiply the top panels by the nuclear density $|\chi(R, t)|^2$, to obtain the total electron-nuclear probability density, shown in Figure 9. It is evident in this graph that there is much less ionization than in the previous case, and the dissociation is slower.

Although the Hartree approximation treats the nuclei quantum mechanically, and therefore allowing tunneling in principle, tunneling and dissociation do not actually occur. The reason for this is clear from the shape of the Hartree potential, plotted in Fig. 10: the Hartree potential essentially retains its initial shape at all times, making very small oscillations near the equilibrium separation. As in the more intense field case, this is due to its uncorrelated treatment of the electron-nuclear system: the electronic wavefunction at any nuclear configuration is always the same, and is best at equilibrium since initially it is determined by

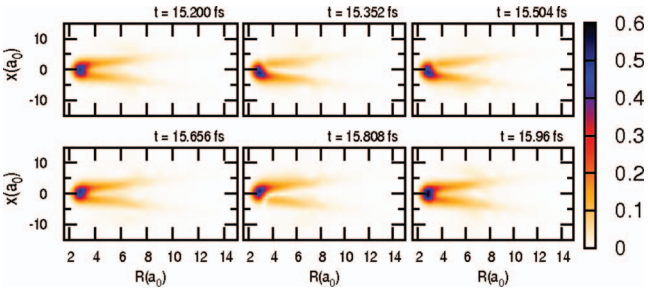

FIG. 9. Snapshots of the total electron-nuclear density at times indicated during an optical cycle, for the H_2^+ molecule subject to the laser-field with the peak $I_2 = 2.5 \times 10^{13}$ W/cm^2.

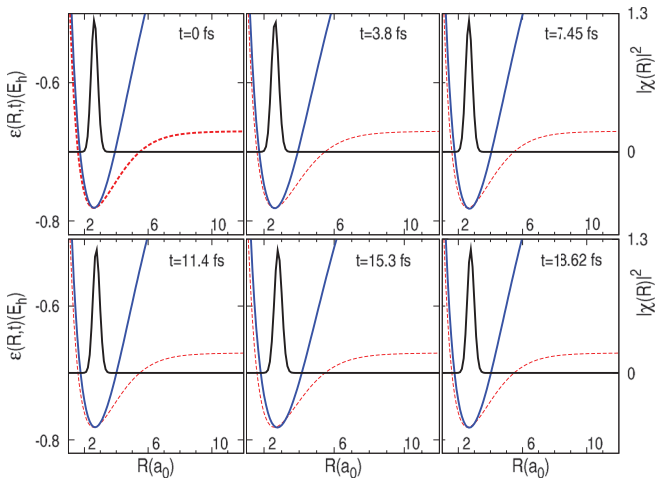

FIG. 10. Snapshots of the time-dependent Hartree nuclear-potential (blue lines) and nuclear density (black) at times indicated, for the H_2^+ molecule subject to the laser-field with the peak intensity $I_1 = 10^{14}$ W/cm^2 $I_2 = 2.5 \times 10^{13}$ W/cm^2. For reference, the ground-state BO surface is shown as the dashed red line.

energy-optimization, from where it does not deviate far, due to the weak field strength. Unlike in the stronger field case, the Hartree surface never opens out. Dissociation via tunneling requires both a quantum mechanical description of the nuclei and an adequate accounting of electron-nuclear correlation.

We do not expect the TDPES to be so different from the BO surfaces in all cases. For example, in the case of field-free vibrational dynamics of the H_2^+ molecule, where we start with a nuclear wavepacket displaced from equilibrium on the ground BO surface, we find the TDPES follows closely the BO surface throughout. The non-adiabatic couplings are weak in this case. The TDPES for field-free dynamics in other systems with stronger non-adiabatic couplings will be published elsewhere.[43]

The purpose of comparing the exact results with these methods (TD-Hartree, Ehrenfest, and exact-Ehrenfest) was primarily to support the conclusions drawn from the exact TDPES regarding the dissociation mechanisms. An interesting question is how well do the more accurate approximate PES's proposed recently (e.g., Ref. 16) compare with the exact TDPES; this will be investigated in the future.

V. CONCLUSIONS

In this paper, we have shown that there exists a rigorous factorization of the exact molecular wavefunction into a nuclear wavefunction and electronic wavefunction, each of which retains the usual probabilistic meaning. The exact nuclear N_n-body density is $|\chi(\underline{\underline{\mathbf{R}}}, t)|^2$ while $|\Phi_{\underline{\underline{\mathbf{R}}}}(\underline{\mathbf{r}}, t)|^2$ represents the conditional probability of finding the electrons at $\underline{\mathbf{r}}$, given the nuclear configuration $\underline{\underline{\mathbf{R}}}$. Equations (28)–(33) are the equations of motion that the electronic wavefunction and nuclear wavefunction satisfy, and show explicitly how the electronic and nuclear systems are exactly coupled. These equations enable the time-dependent potential energy surface (Eq. (32)) and the time-dependent Berry connection (Eq. (33)) to be defined as rigorous concepts, and we have discussed some general properties of them, and of the electron-nuclear coupling operator Eq. (31).

The example of the one-dimensional H_2^+ molecule in an oscillating electric field, solved numerically accurately, demonstrated that the TDPES is a powerful tool to analyze and interpret different types of dissociation processes. By studying the shape and evolution of the TDPES, comparing classical dynamics in this exact potential to the exact quantum dynamics, we were able to distinguish whether the dissociation proceeded via nuclear tunneling or more directly in Coulomb-explosion. For this example, the TDPES is the only potential determining the nuclear dynamics, exactly containing the coupling with electronic dynamics. The example demonstrated the importance of capturing both quantum effects in nuclear motion and electron-nuclear coupling; the Hartree approach, for example, despite treating the nuclei quantum mechanically, was unable to capture dissociation via tunneling as the shape of its potential surface was completely wrong. Thus, the TDPES, and in more general cases than the one studied here, the geometric phase, can be very useful interpretative tools for dynamics. The calculation of a TDPES has quite some history in the strong-field community, and several possible definitions of TDPES have been proposed in the literature. The crucial point of our work is that it provides a *unique* definition of TDPES (unique up to within a gauge transformation): if one wants the TD many-body Schrödinger equation (29) to give the correct N-body density and current density of the nuclei, then the scalar potential and the vector potential *must* be given by Eqs. (32) and (33). There is no choice apart from the gauge. That means that with any advanced technique that yields the TD molecular wavefunction $\Psi(\underline{\mathbf{r}}, \underline{\underline{\mathbf{R}}}, t)$ one can evaluate the TDPES and Berry potential by first calculating the factors from Eqs. (25)–(26) and then evaluating the TDPES and Berry potential from Eqs. (32)–(33).

From a practical point of view, Eqs. (28)–(33) are not easier to solve than the time-dependent Schroedinger equation for the full electron-nuclear system. Rather, they form the rigorous starting point for making approximations, especially for the systematic development of semiclassical approximations. In the large-nuclear mass limit, the electronic equation reduces to Cederbaum's time-dependent BO approximation.[1,18] Taking the classical limit for the nuclei in the large-mass limit, one retrieves the Ehrenfest equations with Berry potential[1] (see also Refs. 48 and 49). Treating the nuclei classically but retaining their finite mass, one finds corrections to the Ehrenfest equations that better account for non-adiabatic transitions.[50] A direction for future research is to capture some nuclear quantum effects by a semiclassical or quasiclassical procedure,[51,52] built on the exact foundational equations presented here. Another direction would be to use the formalism as a possible starting point to develop electron-nuclear correlation functionals in a density-functionalized version of the electron-nuclear problem.[46] A promising route is to develop a time-dependent generalisation of the optimized effective potential scheme proposed in Ref. 20.

ACKNOWLEDGMENTS

Partial support from the National Science Foundation (CHE-1152784) (NTM), from the Deutsche Forschungsgemeinschaft (SFB 762), and from the European Commission (FP7-NMP-CRONOS) is gratefully acknowledged.

[1] A. Abedi, N. T. Maitra, and E. K. U. Gross, Phys. Rev. Lett. **105**, 123002 (2010).
[2] A. D. Bandrauk and H. Kono, "*Molecules in intense laser fields: Nonlinear multiphoton spectroscopy and near-femtosecond to sub-femtosecond (attosecond) dynamics*," in *Advances in MultiPhoton Processes and Spectroscopy*, edited by S. H. Lin, A. A. Villaeys, and Y. Fujimura (World Scientific, Singapore, 2003), Vol. 15, pp. 147–214.
[3] J. P. Marangos, "Molecules in a strong laser field," in *Atoms and Plasmas in Super-Intense Laser Fields*, edited by D. Batani, C. J. Joachain, and S. Martellucci, SIF Conference Proceedings, Vol. 88 (Societ'a Italiana di Fisica, Bologna, 2004), pp. 213–243.
[4] M. F. Kling *et al.* Science **312**, 246 (2006).
[5] W. R. Duncan and O. V. Prezhdo, Annu. Rev. Phys. Chem. **58**, 143 (2007).
[6] C. Rozzi *et al.*, "Quantum coherence controls the charge separation in a prototypical artificial light harvesting system" (unpublished).
[7] S. Chelkowski *et al.*, Phys. Rev. A **54**, 3235 (1996).
[8] F. Martín *et al.*, Science **315**, 629 (2007).
[9] G. K. Paramonov, Chem. Phys. Lett. **411**, 350 (2005).
[10] A. P. Horsfield *et al.*, Rep. Prog. Phys. **69**, 1195 (2006).
[11] M. Ben-Nun *et al.*, J. Phys. Chem. A **104**, 5161 (2000).
[12] A. D. McLachlan, Mol. Phys. **8**, 39 (1964); J. C. Tully, Faraday Discuss. **110**, 407 (1998); J. Chem. Phys. **93**, 1061 (1990); M. Thachuk, M. Yu Ivanov, and D. M. Wardlaw, *ibid.* **105**, 4094 (1996); M. A. L. Marques *et al.*, Comput. Phys. Commun. **151**, 60 (2003).
[13] E. Tapavicza *et al.*, J. Chem. Phys. **129**, 124108 (2008).
[14] O. V. Prezhdo, W. R. Duncan, and V. V. Prezhdo, Prog. Surf. Sci. **84**, 30 (2009).
[15] A. D. Bandrauk and M. Sink, J. Chem. Phys. **74**, 1110 (1981).
[16] H. Kono *et al.*, Chem. Phys. **304**, 203 (2004).
[17] F. Kelkensberg *et al.*, Phys. Chem. Chem. Phys. **13**, 8647 (2011).
[18] L. S. Cederbaum, J. Chem. Phys. **128**, 124101 (2008).
[19] G. Hunter, Int. J. Quantum Chem. **9**, 237 (1975).
[20] N. I. Gidopoulos and E. K. U. Gross, "Electronic non-adiabatic states," e-print arXiv:cond-mat/0502433.
[21] M. V. Berry, Proc. R. Soc. London, Ser. A **392**, 45 (1984).
[22] B. K. Kendrick, J. Phys. Chem. A **107**, 6739 (2003).
[23] R. Resta, J. Phys.: Condens. Matter **12**, R107 (2000).
[24] F. Bouakline, S. C. Althorpe, P. Larregaray, and L. Bonnet, Mol. Phys. **108**, 969 (2010).
[25] S. Althorpe, J. Chem. Phys. **124**, 084105 (2006).
[26] C. A. Mead, Rev. Mod. Phys. **64**, 51 (1992).
[27] M. Born and K. Huang, *Dynamical Theory of Crystal Lattices* (Oxford University Press, New York, 1954).
[28] L. S. Cederbaum, "Born-Oppenheimer approximation and beyond," in *Conical Intersections: Electronic Structure, Dynamics, and Spectroscopy*, Advanced Series in Physical Chemistry Vol. 15, edited by Wolfgang Domcke, David Yarkony, and Horst Köppel (World Scientific, Singapore, 2004), pp. 3–40.
[29] M. Baer, *Beyond Born-Oppenheimer: Conical Intersections and Electronic Nonadiabatic Couplin Terms* (Wiley, 2006).
[30] G. Hunter, Int. J. Quantum Chem. **XIX**, 755–761 (1981).
[31] J. Czub and L. Wolniewicz, Mol. Phys. **36**, 1301 (1978).
[32] I. Barth *et al.*, Chem. Phys. Lett. **481**, 118 (2009).
[33] J. Javanainen, J. Eberly, and Q. Su, Phys. Rev. A **38**, 3430 (1988).
[34] D. G. Lappas, A. Sanpera, J. B. Watson, K. Burnett, P. L. Knight, R. Grobe, and J. H. Eberly, J. Phys. B **29**, L619 (1996).
[35] D. M. Villeneuve, M. Y. Ivanov, and P. B. Corkum, Phys. Rev. A. **54**, 736 (1996).
[36] A. Bandrauk and H. Ngyuen, Phys. Rev. A. **66**, 031401(R) (2002).
[37] T. Kreibich, R. van Leeuwen, and E. K. U. Gross, Chem. Phys. **304**, 183 (2004).
[38] D. G. Lappas and R. van Leeuwen, J. Phys. B **31**, L249 (1998).
[39] M. Lein *et al.*, Phys. Rev. A **65**, 033403 (2002).
[40] T. Kreibich *et al.*, Phys, Rev. Lett. **87**, 103901 (2001).
[41] A. D. Bandrauk and H. Lu, Phys. Rev. A. **72**, 023408 (2005).
[42] J. A. Fleck, J. R. Morris, and M. D. Feit, Appl. Phys. A **10**, 129 (1976).
[43] A. Abedi *et al.*, "Studies of the exact time-dependent potential energy surfaces for field-free non-adiabatic dynamics" (unpublished).
[44] H. D. Meyer, U. Manthe, and L. S. Cederbaum, Chem. Phys. Lett. **165**, 73 (1990).
[45] G. Herzberg and H. C. Longuet-Higgens, Discuss. Faraday Soc. **35**, 77 (1963).
[46] T. Kreibich and E. K. U. Gross, Phys. Rev. Lett. **86**, 2984 (2001).
[47] K. C. Kulander, Phys. Rev. A. **35**, 445 (1987).
[48] V. Krishna, J. Chem. Phys. **126**, 134107 (2007).
[49] Q. Zhang and B. Wu, Phys. Rev. Lett. **97**, 190401 (2006).
[50] A. Abedi, F. Agostini, and E. K. U. Gross, "Exact factorization of the time-dependent electron-nuclear wavefunction: A mixed quantum classical study" (unpublished).
[51] R. Kapral and G. Ciccotti, J. Chem. Phys. **110**, 8919 (1999).
[52] W. H. Miller, J. Phys. Chem. A **113**, 1405 (2009).